REPUBLIC OF AZERBAIJAN

On the rights of the manuscript

ABSTRACT

of the dissertation for the degree of Doctor of Science

IMPACT OF GAMMA RAYS ON ELECTRICAL, FERROELECTRIC AND OPTICAL PROPERTIES OF $TlGa_{1-x}In_xSe_{2(1-x)}S_{2x}$ AND $TlGa_{1-x}In_xSe_2$ SOLID SOLUTIONS

Speciality: 2225.01 Radiation materials science

Field of science: Physics

Applicant: **Famin Tahir oglu Salmanov**

Baku – 2021

The work was performed at Institute of Radiation Problems of Azerbaijan National Academy of Sciences

Scientific advisers: Doctor of physical sciences, professor
Rauf Madat oglu Sardarli

Correspondent member of ANAS, professor
Ogtay Abil oglu Samadov

Official opponents:

Correspondent member of ANAS, professor
Salima Ibrahim gizi Mehdiyava

Doctor of physical sciences, professor
Nizami Mikayil oglu Mehdiyev

Doctor of physical sciences, professor
Cahangir Islam oglu Huseynov

Doctor of physical sciences, associate professor
Sadiyar Soltan oglu Rahimov

Dissertation council **BED 1.21** of Supreme Attestation Commission under the President of the Republic of Azerbaijan operating at Institute of Radiation Problems of Azerbaijan National Academy of Sciences

Chairman of the Dissertation council:
Doctor of physical sciences, associate professor
Rahim Salim oglu Madatov

Scientific secretary of the Dissertation council:
Doctor of philosophy on physics
Muslum Ahmad oglu Mammadov

Chairman of the scientific seminar:
Doctor of physical sciences, associate professor
Matanat Ahmad gizi Mehrabova

GENERAL CHARACTERISTICS OF THE WORK

The actuality of the subject. The widespread practical application of semiconductor materials in various fields of modern technology, including nanotechnology, requires the study of crystals containing radiation defects, various impurities and other heterogeneous crystals. The various types of defects present in crystals have a strong effect on the temperature dependence of the electrical conductivity of the crystal, the dielectric and optical properties, as well as the ion conductivity of the crystals.

One of the most important tasks of modern physics is the study of the laws of composition and structure of new functional and multicomponent materials.The study of such patterns allows the development of a scientific basis for the search and acquisition of new, more efficient semiconductors with predetermined physical properties and to meet the growing demands of microelectronics. The study of solid solutions based on semiconductor compounds is of particular importance because they allow to change the physical parameters. The peculiarity of the structure of solid solutions is that, while maintaining the ideal crystallographic symmetry in these systems, the disorder is caused by the irregular filling of the nodes of the crystal matrix (broadcast irregularity). As a result of anion and cation substitution, depending on the size of the substituting atom in solid solutions, a partial change in the parameters of the elemental nucleus occurs while maintaining the lattice type. In this case, due to the static distribution of atoms in the nodes of the lattice, the transmission sequence of the crystals is broken, and such mixed crystals become analogs of irregular systems.

In addition, by changing the composition of solid solutions, it is possible to obtain information about the photoelectric, dielectric and optical properties of the semiconductor material studied, as well as the levels of the semiconductor located within the forbidden band.

Our research shows that in these compounds, in addition to the zone-zone conductivity, there is a jumping conductivity. This shows that the crystals we measure have an irregular structure. This permeability is observed in a wide temperature range over the localized levels in our compounds. This indicates that the solid solutions under study have an irregular structure.

Specific features are manifested in the energy spectra of irregular materials: the mechanism of relaxation processes of dielectric properties in these materials changes, specific features appear in the process of the charge carrier.

Superions, which form a special class, have attracted large groups of researchers in recent years. One of the main differences of superions is that they have anomalously high ionic conductivity. In superions, the value of ionic conductivity is in the order characteristic of electrolytes. Thus, we are talking about substances with unique hybrid properties - liquid alloys or mixtures, mechanically solid and elastic solids. Superion crystals can be in two different phases, which are qualitatively different from each other. These crystals have the properties of ordinary ionic crystals below the critical temperature (dielectric phase), and above the critical temperature they have the properties of a special state-superion (electrolyte state). Crystals that have these properties are called superionic conductors.

The method of impedance spectroscopy is widely used in fundamental and applied research.

The method used to study the total conductivity of a crystal is the impedance spectroscopy method. This method allows you to determine the full value of resistance and capacitance over a wide frequency range. That is, ion conduction is the only experimental method that studies the relaxation processes in a crystal. This method allows you to model the process of building an equivalent circuit at the expense of the hodographs observed in the crystals. This method is one of the main research methods of superion permeability.

The method of impedance spectroscopy is used in electrochemical and materials science studies, more precisely, in the case of charge carrier, events at interfacial boundaries, etc. plays a major role in ongoing research.

For this purpose, the production of layered and chain $TlGaSe_2$, $TlInS_2$, $TlInSe_2$ compounds and solid solutions based on them is practically important in terms of the effect of various mixtures (impurities) on the physical parameters of promising compounds and the management of these parameters in a wide homogeneous field.

The purpose of the dissertation: The main purpose of the dissertation is to study the characteristics of the effect of gamma rays on the dielectric, optical and impedance spectra over a wide frequency and temperature range of solid solutions $TlGa_{1-x}In_xSe_{2(1-x)}S_{2x}$and $TlGa_{1-x}In_xSe_2$.

The following issues had to be addressed in order to achieve the set goal:

- Synthesis of solid solutions of $TlGa_{1-x}In_xSe_{2(1-x)}S_{2x}$and $TlGa_{1-x}In_xSe_2$systems and cultivation of single crystals by selecting the appropriate technological mode;

- Study of the effect of γ-rays on the characteristics of the leakage conductivity of solid solutions of $TlGa_{1-x}In_xSe_{2(1-x)}S_{2x}$and $TlGa_{1-x}In_xSe_2$ systems in the wide temperature (100-450 K) and wide frequency (20-106 Hz) regions;

- study of current density and Pul-Frenkel effect of solid solutions of $TlGa_{1-x}In_xSe_{2(1-x)}S_{2x}$ and $TlGa_{1-x}In_xSe_2$ systems irradiated with gamma quanta under the influence of the field;

- Study of the effect of gamma rays on the superionic conductivity of solid solutions of $TlGa_{1-x}In_xSe_{2(1-x)}S_{2x}$ and $TlGa_{1-x}In_xSe_2$ systems;

- Study of the effect of gamma rays on the impedance spectra of solid solutions of $TlGa_{1-x}In_xSe_{2(1-x)}S_{2x}$ and $TlGa_{1-x}In_xSe_2$ systems in the wide temperature (100-450 K) and wide frequency (20-106 Hz) regions;

- Study of the effect of gamma rays on the optical spectra of solid solutions of the system $TlGa_{1-x}In_xSe_{2(1-x)}S_{2x}$ and $TlGa_{1-x}In_xSe_2$ in the area of the fundamental absorption band;

- Study of surface processes of solid solutions of $TlGa_{1-x}In_xSe_{2(1-x)}S_{2x}$ and $TlGa_{1-x}In_xSe_2$ systems irradiated with gamma quanta under the Atomic Force Microscope.

- Study of surface processes of solid solutions of $TlGa_{1-x}In_xSe_{2(1-x)}S_{2x}$, $TlGa_{1-x}In_xSe_2$ system and $TlInS_2$ <0.1%V> irradiated with γ quanta under the Atomic Force Microscope.

Research methods:

The $TlGaSe_2$, $TlInS_2$ and $TlInSe_2$compounds and single crystals of their solid solutions, which were the objects of research, were grown by the Bridgman-Stockbarger method. The synthesized substance (5.0-10 g) is filled into a quartz ampoule and is airless. After determining the temperature of growth and evaporation of the crystal according to the state diagram and the selected composition, the tem-

perature of the melting zone in the electric furnace is collected according to the selected temperature and automatically stabilized by thermal regulator (RIF-101), the temperature of the brewing zone is also stabilized by a thermostat after it has been assembled in accordance with the selected temperature. After stabilization for 2-3 hours, the Pt-Pt / Rh thermocouple connected to a 2-coordinate recording device from the point "0" to the end of the brewing zone is released into the furnace at a speed of 0.2 cm / min. The temperature of the brewing zone was selected in the order of ≈55-60% of the melting point of the substance. Once the required temperature gradient and the temperature in the zone have been found to match the selected temperature, the substance to be grown is combined with a quartz ampoule into a moving mechanism and introduced into the furnace. After stabilization for 1.5-2 hours, the container is set in motion and thus the crystallization process begins. The growth rate of the solid solutions used in the study was 1-1.5 mm / h.

Measurements of electrical conductivity were carried out by the four-probe method, in the direction perpendicular to the tetrogonal "c" axis, in a nitrogen cryostat, in the mode of quasi-stationary continuous heating (cooling) of the crystal at a speed of ≈ 0.1 K / min. Electrical conductivity studies were performed on a digital imitation E7-25 measuring device. Electrical conductivity was measured over a wide temperature (100-450K) and frequency range (25Hz-1MHs).

Volt-Ampere characteristics of the samples were studied in the temperature range 90-300 K in order to obtain information about the current transfer mechanism in semiconductor materials. A direct current source and a B7-30 electrometer were used during the measurement. Silver paste was drawn in the direction perpendicular and parallel to the crystallographic "c" axis of the samples, such as current contacts. The degree of ohmicity of the current contacts was determined by the characteristic graph.

In optical measurements, the emission and reflection spectra from the surface of the transparent plates cut along the planes of the crystal (001) were measured. In these samples, the emission spec-

trum was measured. Measurement of light falling at about 12^0 normal angles was performed with the help of a spectrophotometer "specord 210". Measurements were performed at room temperature with E⊥C polarization. The resolution of the spectrometer is 10 nm. The wavelength of the spectrometer was ± 3 nm. Therefore, E_g is calculated with better accuracy up to ± 0.0004 eV.

Impedance spectroscopy was also used to study the electrophysical processes occurring in the metal contacts of ion-conducting materials.

The surface processes of the materials studied in the study were also studied. The study of surface processes is based on the study of the local interactions between the surface of the sample and the probe when they are brought closer together. The main methods of studying the probe microscope are scanning tunneling microscope and atomic force microscope.

A sharp conducting needle is used as a probe in a scanning tunnel microscope. An operating voltage is applied between the tip of the needle and the sample, and when the tip is brought closer to the sample to about 0.5-1.0 nm, the electrons in the sample begin to form a tunnel upwards or vice versa, depending on the polarization of the working voltage. Based on the data obtained from the measurement of tunneling current in the scanning tunneling microscope, the topography is visualized. The sample and the tip must be semiconductor or conductive to record tunnel current. When the atoms that make up the tip coincide with the wave functions, a scanning needle and a tunneling current of charge carriers are formed on the surface. It should be noted that the technique used in the scanning tunneling microscope does not describe non-conductive materials.

The main scientific provisions submitted for defense:

1. The electrical conductivity of $TlGa_{1-x}In_xSe_{2(1-x)}S_{2x}$and $TlGa_{1-x}In_xSe_2$ systemic solutions irradiated with γ-quanta in the temperature range of 100-300 K has been determined and explained in terms of the Mott approximation.

2. It has been determined that the current in the nonlinear part of the Volt-Ampere characteristics of solid solutions of $TlGa_{1-x}In_xSe_{2(1-x)}S_{2x}$

exposed to γ-radiation is due to the weak field effect and is explained in the framework of Poole-Frenkel's thermal-field theory.

3. Temperature dependence of the electrical conductivity of samples of solid solutions of the system $TlGa_{1-x}In_xSe_{2(1-x)}S_{2x}$and $TlGa_{1-x}In_xSe_2$ irradiated with γ-quanta, the jump-shaped increase observed (σ (T)) at room temperatures is due to the transition of the crystal to the superion phase.

4. The frequency dispersion of the dielectric constant of dielectric solids of the system $TlGa_{1-x}In_xSe_{2(1-x)}S_{2x}$and $TlGa_{1-x}In_xSe_2$irradiated with γ-quanta and the relaxor properties of the dielectric loss angle were determined. It has been shown that the charge-carrying mechanism bounces near the Fermi level at 1^{05} Hz. The parameters of a given conduction mechanism were evaluated before and after γ radiation. It has been found that the increase in jumping conductivity at T = 350K and 1^{06} Hz is due to the transition of the system to superion.

5. The study of complex impedance spectra in solid solutions of the system T $TlGa_{1-x}In_xSe_{2(1-x)}S_{2x}$and $TlGa_{1-x}In_xSe_2$ revealed that after γ-irradiation Warburg diffusion impedance is formed.

6. In γ-irradiated $TlGa_{1-x}In_xSe_{2(1-x)}S_{2x}$and $TlGa_{1-x}In_xSe_2$ systemic solid solutions at room temperature, concentration dependence of the bandwidth of the forbidden band on the straight and across of the reflection and emission spectra in the spectral range of 400-1100 nm has been determined.

7. As a result of the study of the electrical conductivity of the crystal $TlInS_2$<V> under the influence of a changing electric field, it was determined that the jump conductivity is carried out below the Burns (T_d) temperature. Thermoactivated conduction up to the Vogel-Fulcher temperature (T_f) and inactivation jumping conduction below T_f is important.

8. Atomic Force Microscopy of $TlInS_2$ and $TlInS_2$ <0.1%V>crystals and solid solutions of $TlGa_{1-x}In_xSe_2$ revealed that the effects of radiation increase the saturation of nanoscale clusters, increase the ability of molecules to dissociate, and lead to the formation of critical embryos.

Scientific novelty of the research:

1.The jumping electrical conductivity of $TlGa_{1-x}In_xSe_{2(1-x)}S_{2x}$ and $TlGa_{1-x}In_xSe_2$ systemic solutions irradiated with γ-quanta in the temperature range of 300-100 K has been determined and explained in terms of the Mott approximation.

2. It was found that the current in the nonlinear part of the Volt-Ampere characteristics of solid solutions of the $TlGa_{1-x}In_xSe_{2(1-x)}S_{2x}$ system exposed to γ-radiation is due to the weak field effect and is explained in the framework of Poole-Frenkel's heat-field theory.

3. It was found that the temperature dependence of the electrical conductivity of $TlGa_{1-x}In_xSe_{2(1-x)}S_{2x}$ and $TlGa_{1-x}In_xSe_2$ system solid solution samples irradiated with γ-quanta at room temperature above room temperature (σ (T)) is related to the transition to the superion state of the crystal.

4. The study of complex impedance spectra in systemic solid solutions $TlGa_{1-x}In_xSe_{2(1-x)}S_{2x}$ and $TlGa_{1-x}In_xSe_2$ revealed that after γ-irradiation Warburg diffusion impedance is formed.

5. Frequency dispersion of dielectric constant and relaxor properties of dielectric loss angle of $TlGa_{1-x}In_xSe_{2(1-x)}S_{2x}$ and $TlGa_{1-x}In_xSe_2$ system solid solutions irradiated with γ-quanta were determined. It has been shown that the charge-carrying mechanism bounces near the Fermi level at 10^5 Hz. It was found that the increase in jumping conductivity at T = 350K and 10^6 Hz is due to the transition of the system to superion.

6. In γ-irradiated $TlGa_{1-x}In_xSe_{2(1-x)}S_{2x}$and $TlGa_{1-x}In_xSe_2$ systemic solid solutions at room temperature, concentration dependence of the bandwidth of the forbidden band on the straight and across of the reflection and emission spectra in the spectral range of 400-1100 nm has been determined. It was found that in solid solutions $TlGa_{1-x}In_xSe_{2(1-x)}S_{2x}$ the width of the forbidden zone increases with increasing concentration and radiation dose, while in solid solution $TlGa_{1-x}In_xSe_2$ the width of the forbidden zone decreases after irradiation.

7. As a result of the study of the electrical conductivity of the crystal $TlInS_2$<V> under the influence of a changing electric field, it

was determined that the jump conductivity is carried out below the Burns (T_d) temperature. Thermoactivated conduction up to the Vogel-Fulcher temperature (T_f) and inactivation jumping conduction below T_f is important.

8. Atomic Force Microscopy of $TlInS_2$ and $TlInS_2$ <0.1%V>crystals and solid solutions of $TlGa_{1-x}In_xSe_2$ revealed that the effects of radiation increase the saturation of nanoscale clusters, increase the ability of molecules to dissociate, and lead to the formation of critical embryos.

Practical significance of the work:

The main results that can be used in the practice obtained in the dissertation: can be used as memory elements and converters, micro batteries, supercapacitors, ionizers, suitable material for gamma sensor.

Studies have shown that γ-irradiated $TlGa_{1-x}In_xSe_{2(1-x)}S_{2x}$ and $TlGa_{1-x}In_xSe_2$ systemic solid solutions at room temperature, from the straight and across of the reflection and emission spectra in the spectral range of 400-1100 nm, the width of the forbidden band varies with increasing radiation dose. Due to this feature, these crystals cn be used as photochromic crystals.

Approbation of work. The results of the dissertation were presented at the following conferences: "VII Eurasian conference Nuclear Science and its Application, (Baku, 2014); "Fizikanın müasir problemləri VIII Respublika konfransı" (Bakı, 2014); "BDU-nun Fizika Problemləri İnstitutunun yaradılmasının 10 illiyinə həsr olunmuş "Fizikanın aktual problemləri" IX respublika elmi konfransının materialları" (Bakı 2016); "International youth forum, Integration processes of the world science in the 21th century" (Ganja, Azerbaijan 2016); Международная конференция, посвященная 60-летию Института физики ДНЦРАНи 110-летию Х.И. Амирханова, «Фазовые переходы, критические и нелинеиные явления в конденсированных средах» (Махачкала 2017); "XXI Всероссийскую конференцию по физике сегнетоэлектриков (ВКС – XXI)" (Казан 2017); "International Conference on Nanotechnology: Fundamentals and Applications Toronto, Ontario" (Can-

ada 2017); 11-я Международная конференция «Ядерная и радиационная физика» Международная конференция «Ядро-2017» (Алматы2017); “XIV Международной научной конференции«Молодежь в науке-2.0′17» (Минск 2017); «Третий междисциплинарный молодежный научный форум с международным участием «Новые материалы» (Москва 2017). Международный форум молодых ученых «BURABAY FORUM: (Qazaxıstan,Astana -2018.) ; Международный научный форум «Ядерная наука и технологии» (Казахстан,Алматы 2019); Материалы XXIV международной конференции, (г. Воронеж, 2019) «Пятый междисциплинарный молодежный научный форум с международным участием «Новые материалы» (Москва 2019)

Name of the organization where the dissertation work is carried out: "Laboratory of radiation physics of segnetoelectrics" of the Institute of Radiation Problems of the Azerbaijan National Academy of Sciences

Publications. 23 scientific works, including 18 articles, 5 conference materials were published in national and foreign scientific journals on the topic of the dissertation.

The structure and scope of the dissertation. The dissertation consists of an introduction, six chapters, main results and a list of references. The work is commented on contains 89 figures and 10 tables. The list of cited literature includes 89 figures, 10 tables and a total of 350,806 symbols were used in the submitted dissertation work.

SUMMARY OF THE WORK

The introduction substantiates the relevance of the topic of the dissertation, indicates the purpose of the work, scientific novelty, practical importance, provides information about the main provisions, the degree of approbation, publications, as well as briefly explains the main content of the work by chapters.

Chapter I of the dissertation analyzes the literature on the broadcast phase transitions in ferroelectrics of the type $TlB^3C_2^6$, the effect of impurities on these phase transitions, as well as the electrophysical properties of $TlGaSe_2$, $TlGaS_2$ and $TlInS_2$ crystals and solid solutions formed between them. In addition, Chapter I examines the literature on solid-state electrolytes, superionic conductors, the conditions of observation of quantum measurement effects, as well as the optical spectra of $TlB^3C_2^6$ crystals.

Chapter II of the dissertation describes the synthesis of the studied materials and the method of growing monocrystals. In addition, this chapter presents the scheme of devices for the study of electrical and dielectric properties and the principle of their operation, the methodology of research on the effects of γ-rays. In addition, the method of studying the micro-relief of the surface of crystals through an atomic force microscope, the method of measuring the impedance spectrum were explained.

Chapter III of the dissertation the system $TlGa_{1-x}In_xSe_{2(1-x)}S_{2x}$ (x=0; 0,1; 0,2; 0,3; 0,7; 0,8; 0,9; 1,0) irradiated with γ-quanta The results of the study of temperature dependence of electrical conductivity and dielectric constant, Volt-Ampere characteristic, impedance spectroscopy in the temperature range of 100-450K and frequency range of $25\text{-}10^6$ Hs of solid solutions are presented.

Solid solutions of $TlGa_{1-x}In_xSe_{2(1-x)}S_{2x}$ and $TlGa_{1-x}In_xSe_2$ systems belong to the class of layered semiconductors combined in the general formula $A^{III}B^{III}C^{VI}_2$. The development features of modern solid state physics and solid state electronics are based on the use of new physical properties based on the properties of the material due to structural irregularities. If the ideal cryptographic symmetry is main-

tained in the insertion of the nodes of the structural matrix, the filling of these nodes, the electron spins, and so on. may be irregularities in the orientation due to the violation of periodicity. Irregular materials are a broad class of objects in which properties are observed in the energy spectrum. In such materials, the mechanism of relaxation processes of dielectric properties changes, characteristic features are observed in the process of charge-carrying.

Among the anisotropic crystals that can be combined in the general formula $TlB^{111}C^{VI}_2$, crystals with a chain and layered structure have a special place. These compounds show high sensitivity in the infrared, visible and X-ray spectral regions. Due to this feature of the compounds, in optoelectronic systems, photoresistors, photodetectors, X-ray detectors, nuclear detectors and. s. used as functional elements.

In addition, the effects of composition, structure, and γ-radiation on the electrical conductivity of the sections in the phase diagrams of the binary systems $TlGa_{1-x}In_xSe_{2(1-x)}S_{2x}$ were studied. As an object of study, the choice of special binary systems can be explained by the following factors: For $TlGa_{1-x}In_xSe_{2(1-x)}S_{2x}$ systems it is important to note the similarity of the monoclinic structure and the ionic radii of the elements (R_{In3+}=0,081nm, R_{Ga3+}= 0.062 nm, R_{Se2-}=0.198 nm, R_{S2-}= 0.184 nm). This is consistent with Holdmit's law, in which the presence of solid solution substitutions over a wide range of composition and temperature in multicomponent compounds is high.

The $TlGa_{1-x}In_xSe_{2(1-x)}S_{2x}$ (x=0; 0,1; 0,2; 0,3; 0,7;0,8; 0,9; 1,0) system irradiated with γ quanta studied the properties of the conductivity of solid solutions in the temperature range of 100-300K, and the effect of γ-rays on these properties was studied. The temperature dependence of the electrical conductivity of solid solutions of the $TlGa_{1-x}In_xSe_{2(1-x)}S_{2x}$ (x=0; 0,1; 0,9;1,0) system in Arrhenius coordinates is given in Figure 1

According to the results of the study of the temperature dependence of the electrical conductivity of the solid solutions of the system $TlGa_{1-x}In_xSe_{2(1-x)}S_{2x}$ (x=0; 0,1; 0,2; 0,3; 0,7;0,8; 0,9; 1,0) in

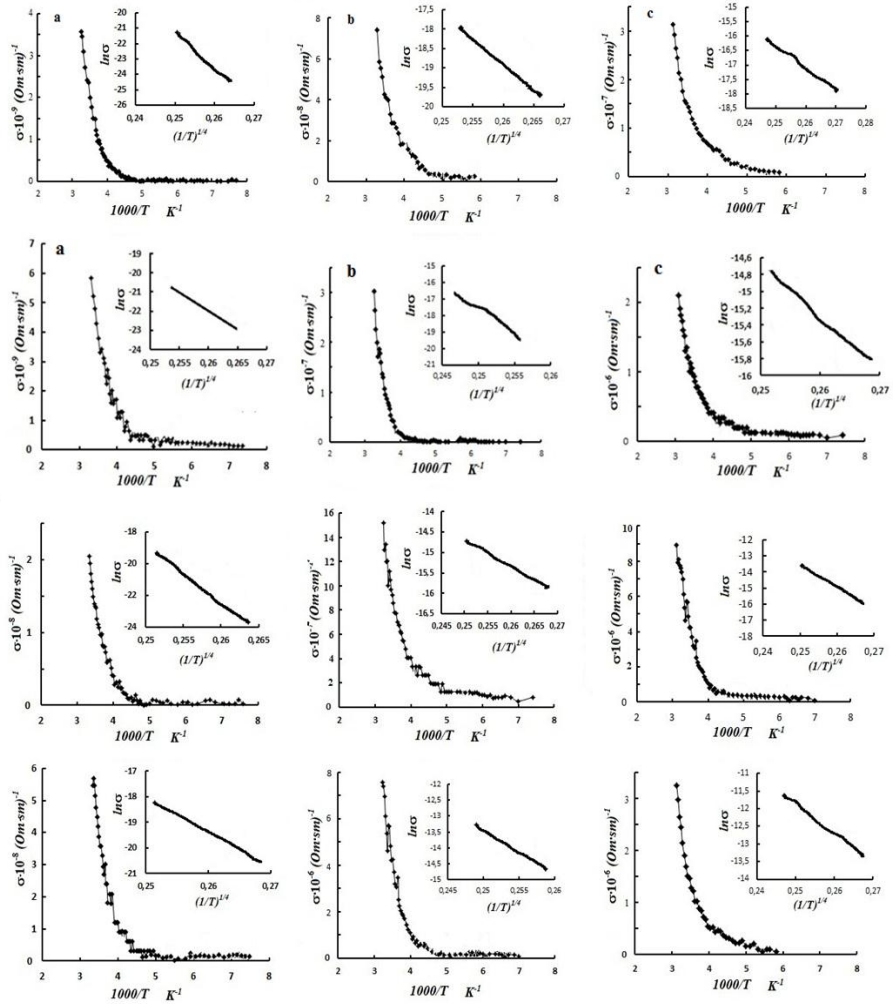

Figure 1. Temperature dependence of the electrical conductivity of $TlGa_{1-x}In_xSe_{2(1-x)}S_{2x}$ (x=0; 0.1; 0.2; 0.3) solid solutions irradiated with γ-quanta. The appendix on the figure shows the dependence of ln σ on $T^{-1/4}$ in Mott coordinates. (a-0 MGy; b-0,25 MGy; c- 0,75 MGy)

the temperature range 100-300 K, the temperature and frequency intervals of the presence of bounce conductivity were determined before and after different doses of radiation.

It has been shown that there are two parts to the change in the specific conductivity of the studied solid solutions from the temperature dependence of the electrical conductivity.

Thus, the temperature range of dependence 175 ÷240 K is exponential. In the specified temperature range, the conductivity of heat-activated charge carriers in the permissible zone is predominant. With a further decrease in temperature, a decrease in the concentration of impurity carriers is observed. Thus, values of temperatures below 175 K for the solid solution samples under study are the freezing zones of the charge carriers. In the temperature regions of 175 <T <240 K, the experimental points are collected in a straight line at the coordinates determined by the dependence of $ln\sigma$ on $T^{1/4}$ in Mott coordinates. This allows us to say that in the specified temperature range, the transport of a charge carrying in a solid solution of $TlGa_{1-x}In_xSe_{2(1-x)}S_{2x}$(x=0; 0,1; 0,9; 1,0) in a non-radiated and irradiated energy is carried out by means of jumping conductivity in localized cases located in a narrow energy band near the Fermi level.

Additional reasons specific to the jumping nature of conduction have been considered. Conductivity parameters based on the Mott approximation: Density of localized conditions near the Fermi level (N_F), concentration of deep traps (N_t), energy difference of localized conditions near the Fermi level (ΔE) as well as values of average length of carriers jumps (R) calculated, dose and composition dependency graphs have been established (Figure 2). The dose-dependence of the jumping conductivity parameters for the studied solid solutions varies significantly in the solution region and depending on the γ-radiation dose compared to the extraneous components. Additional causes leading to localization of energy states in solid solutions have been considered. In the case of a solid solution of $TlGa_{1-x}In_xSe_{2(1-x)}S_{2x}$, additional causes for the formation of defects and, as a result, for the emergence of new localized cases of energy falling within the forbidden price range in the ideal crystal were considered.

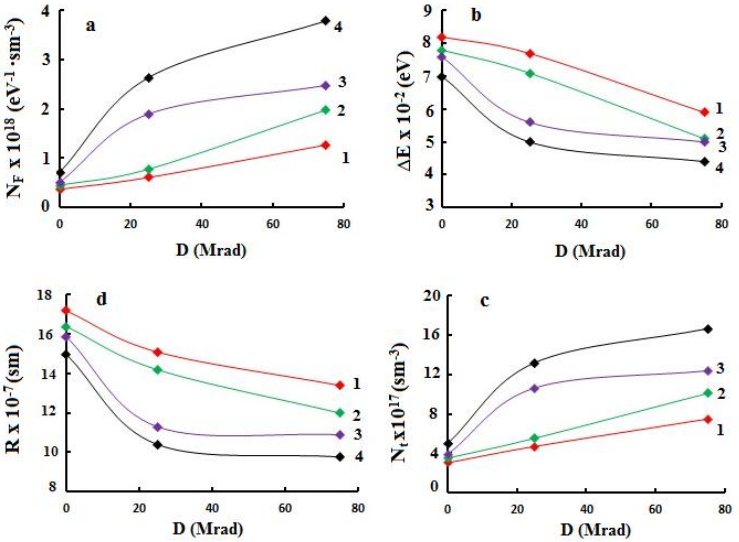

Figure 2. Near the Fermi level of solid solutions of $TlGa_{1-x}In_xSe_{2(1-x)}S_{2x}$ (1-x=0; 2-x=0,1; 3-x=0,2; 4-x=0,3;): a - density of localized cases (N_F), b - energy scattering of localized cases (□E), c - concentration of deep traps (N_t), d - dependence of the length of the jump (R) on the concentration and radiation dose.

The concentration of defects in layered and chain crystals exceeds 10^{18} cm^{-3}. The presence of such a large number of defects is explained by the high density of states near the Fermi level. The reason for the structural defect may be the presence of a large homogeneous region of crystals of group $A^3B^3C^6_2$, reaching 6-8 mol.%. In the homogeneity region, the segregation coefficient is smaller than the unit, so there is a high probability that the composition in the solid solution will deviate from stoichiometry during the growing of single crystals (monocrystalline growth). This, in turn, can lead to a large number of defects in the combination of layers, vacancies and dislocations. Traps created by various defects in the crystals play a key role in the phenomena of charge carrying. The activation energy, which determines the width of the energy band at which jumps of the

charge carriers near the Fermi level, represents virtually the entire electrical conductivity of the crystal.

In the case of a solid solution of $TlGa_{1-x}In_xSe_{2(1-x)}S_{2x}$, the following additional causes of defects can be given, which lead to additional irregularities and, consequently, to the emergence of new energetic localized states of energy falling within the forbidden values range in the ideal crystal:

- the transmission invariance of the crystal lattice is violated, ie the equivalent nodes of the crystal lattice are captured by non-equivalent atoms;

- the presence of microparticles of other phases in the solid solution, such as TlSe, InSe, $TlInTe_2$ and other micro-embryos of other phases;

- Presence of anti-structural defects in the structure of the solid solution, caused by partial substitution of cations In^{3+}, Ga^{3+}, Tl^{1+}, Tl^{3+};

- there is a high probability of position irregularity. This is because in multicomponent solid solutions, one sublattice is ordered (Tl^{1+} sublattice), and in the second sublattice, the atoms alternate chaotically at the nodes of the chain.

Undoubtedly, the above-mentioned types of irregularities contribute to the irregularity of the structure, which leads to the localization of electron states near the Fermi level [17]

This chapter also covers $TlGa_{1-x}In_xSe_{2(1-x)}S_{2x}$ (0; 0,1; 0,2; 0,3; 0,4; 0,6; 0,7; 0,8; 0,9; 1,0), the Volt-Ampere characteristics of solid solutions in the system were studied in the temperature range of 200 ÷ 300 K and in the range of 0 ÷ 3000 V / cm value of the external electric field, both before and after irradiation of 0.75 MGy.

The levels of ionization in semiconductors, dielectrics and their compounds due to the effects of temperature and strong electric field have been theoretically investigated by Frenkel. That is why the increase in the electrical conductivity of these materials under the influence of the electric field is explained by Frenkel's thermoelectron ionization. The increase in electrical conductivity in the strong electric field by the exponential law in the form $\sigma = \sigma_0 e^{\alpha E}$ is shown by

Pool. First of all, it should be noted that Frenkel's thermoelectron ionization is not realized at the electrode, but at the entire volume of the semiconductor and dielectric. The Pool-Frenkel effect has been studied theoretically in many studies and has been found experimentally in semiconductors, dielectrics and compounds based on them.

Due to the rupture of bonds or their reconstruction in semiconductors, there are a large number of traps, ie, valence-alternative defects, as well as the formation of donor and acceptor-type defects with the same concentration, in this case, the donor centers convert the electrical conductivity into the Pool-Frenkel conduction. The essence of the Pool-Frenkel effect is that a decrease in the level of activation energy in the electric field leads to an increase in the current-dependent concentration of dielectrics and semiconductors.

Table.1

Pre-radiation and post-radiation values of parameters calculated within the Pool-Frenkel effect. T = 250

Tərkib $TlGa_{1-x}In_xSe_{2(1-x)}S_{2x}$	radiation	$\beta(sm/V)^{1/2}$	λ (sm)	x_m (sm)	N_t (sm^{-3})
x=1	0 MGy				
	0,75 MGy	0.032	$5,13 \times 10^{-6}$	$1,28 \times 10^{-6}$	5.96×10^{16}
x=0,9	0 MGy	0.027	$4,27 \times 10^{-6}$	1.25×10^{-6}	6.46×10^{16}
	0,75 MGy	0.023	$3,19 \times 10^{-6}$	1.15×10^{-6}	$8,29 \times 10^{16}$
x=0,8	0 MGy	0.012	2.6×10^{-6}	1.13×10^{-6}	$8,66 \times 10^{16}$
	0,75 MGy	0,008	1.1×10^{-6}	9.58×10^{-7}	$1,42 \times 10^{17}$

$TlGa_{1-x}In_xSe_{2(1-x)}S_{2x}$(0; 0,1; 0,2; 0,3; 0,4; 0,6; 0,7; 0,8; 0,9; 1,0) solid solutions that have not been irradiated and exposed to 0.75 MGy radiation, Volt-Ampere characteristics at different temperatures have been studied.According to the experimental results obtained, there are linear and nonlinear ($J \sim U^n$) parts in the Volt-Ampere characteristic at different temperatures and at different electric field val-

ues. As the temperature increases, the ohmic region decreases, and the transition voltage in the quadratic region shifts to smaller values. Such an increase is due to an increase in the concentration of charge carriers.

Analysis of experimental data showed that the dependence of σ on E in solid solutions $TlGa_{1-x}In_xSe_{2(1-x)}S_{2x}$ (0; 0,1; 0,2; 0,3; 0,4; 0,6; 0,7; 0,8; 0,9; 1,0) before and after radiation in a strong electric field ($3 \cdot 10^3$ V/sm) is well described by the Frenkel formula.

Analysis of experimental data showed that the dependence of σ on E in solid solutions $TlGa_{1-x}In_xSe_{2(1-x)}S_{2x}$ (0; 0,1; 0,2; 0,3; 0,4; 0,6; 0,7; 0,8; 0,9; 1,0) before and after radiation in a strong electric field ($3 \cdot 10^3$ V/sm) is well described by the Frenkel formula.

Based on experimental data, lgσ-E and lgσ-$E^{1/2}$ dependencies were established for solid solutions of $TlGa_{1-x}In_xSe_{2(1-x)}S_{2x}$(0; 0,1; 0,2; 0,3; 0,4; 0,6; 0,7; 0,8; 0,9; 1,0).

It is shown that the line of $\lg\sigma - \sqrt{E}$ coordinates corresponds to the dependence. This is well consistent with the theoretical expression of the β-Frenkel coefficient. Analyzing the dependence of β on the inverse of the temperature, it appears that the relationship between these quantities is a straight line (Figure 3). At the same time, it was determined that the temperature dependence of the x-Frenkel coefficient determined from the dependence lnσ ($E^{1/2}$) is subject to the expression $\beta = \frac{\sqrt{e^3}}{kT\sqrt{\pi\varepsilon\varepsilon_0}}$, and the exploration of the line β~10^3/T passes through the origin. In solid solutions $TlGa_{1-x}In_xSe_{2(1-x)}S_{2x}$ (0; 0,1; 0,2; 0,3; 0,4; 0,6; 0,7; 0,8; 0,9; 1,0) at a temperature range of 200÷300K, taking into account the results of electrical conductivity in a strong electric field, the length of the free path (λ), the Frenkel coefficient (β) and the distance from the traps to the maximum potential wall (x_m), it is also possible to calculate the concentration (N_t) of the ionized centers. The comparative values before and after irradiation are given in Table 1 for comparison.

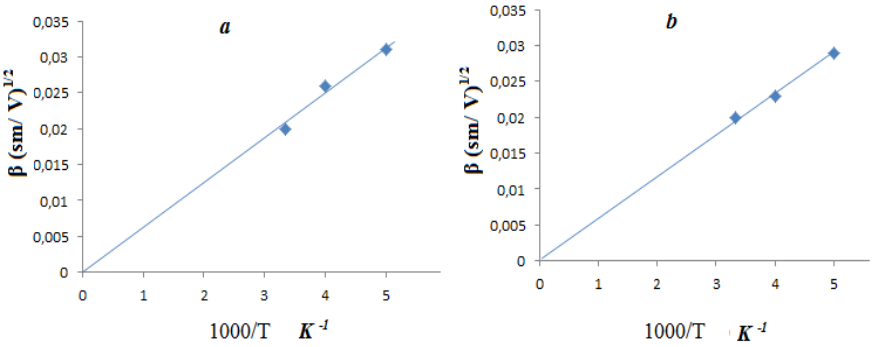

Figure 3. Temperature inverse dependence (a-0 MGy, b-0,75 MGy) of β-Frenkel coefficient for solid solution $TlGa_{1-x}In_xSe_{2(1-x)}S_{2x}$(x=0.9)

It was found that after irradiation at a dose of 0.75 MGy in solid solutions $(TlGaSe_2)_{1-x}(TlInS_2)_x$ (0; 0,1; 0,2; 0,3; 0,4; 0,6; 0,7; 0,8; 0,9; 1,0), the value of the current decreases with respect to the pre-irradiation value, and the value of the transition voltage from the ohmic region to the quadratic region increases. This causes the ohmic region observed in the VAC to shift towards the high voltage region. In the strong electric field of solid solutions of radiation-exposed $(TlGaSe_2)_{1-x}(TlInS_2)_x$ (0; 0,1; 0,2; 0,3; 0,4; 0,6; 0,7; 0,8; 0,9; 1,0), the current in the nonlinear part of the Volt-Ampere characteristics is due to the weak field effect and is explained in the context of Poole–Frenkel's thermal-field theory. The increase in the value of electrical conductivity (σ) in the electric field is explained by Frenkel's thermoelectron ionization, which allows to determine the concentration of traps (N_t), the length of the free path (λ), the Frenkel coefficient (β) and the distance from the traps to the maximum potential wall (x_m).

It has been shown that the concentration of ionization centers due to radiation defects after gamma radiation increases. It was found that the nonlinear part of the Volt-Ampere characteristic is conditioned by the weak field effect, taking into account the heat-field

Pool-Frenkel effect in the $\sigma \sim (E^{1/2})$ dependences of solid solutions $TlGa_{1-x}In_xSe_{2(1-x)}S_{2x}$ (0; 0,1; 0,2; 0,3; 0,4; 0,6; 0,7; 0,8; 0,9; 1,0).

Also in this chapter**,** the ionic conductivity properties of non-irradiated and γ-quantum irradiated $TlGa_{1-x}In_xSe_{2(1-x)}S_{2x}$ (0; 0,1; 0,2; 0,3; 0,4; 0,6; 0,7; 0,8; 0,9; 1,0) systemic solid solutions in the temperature range 100-450K were studied.

Based on the analysis of the literature, the theory of phase transition induced by an electric field to the state of ionic conductivity is based on the important role of the interaction of Frenkel defects in the crystal and the effect of the electric field on the energy of formation of these defects. One of the consequences of the irregularity in ionic conductivity crystals is the increase in the share of ion accumulation in the electrical conductivity of the crystal during electrical measurements, in which case the share of ion accumulation exceeds the electron accumulation by several orders of magnitude.

One of the main factors in the formation of ionic conductivity in solid solutions is the dependence of the structural properties of the substance:

- the number of displaced ions in the elementary lattice of the crystal must be greater than the total number of mobilions;

- There must be "small channels" directly in the crystal lattice for the ions to move. If there were no such small channels, it would be possible for charged particles to move inside one or more elementary lattices.

One of the crystallochemical conditions for ionic conductivity is that the distance between the anion and the cation must be greater than the sum of their ionic radii, creating geometric possibilities for their mutual displacement. Another condition is the presence of Pb^{2+}, Bi^{3+}, Tl^{+}, etc. in the crystalline structure, that is, the presence of highly polarized cations or highly polarized structural elements.

Depending on the temperature dependence of the electrical conductivity of samples exposed to radiation at doses of 0, 0.25 and 0.75 MGy at temperatures above room temperature, it was found that the value of conductivity increased several times at a certain critical temperature. Such a characteristic increase in conductivity indicates

that ionic conductivity predominates at temperatures above that critical temperature. One of the facts showing the existence of ionic conductivity is that in the temperature-dependence curve of electrical conductivity, the linear regularity of the 1/T dependence of ln(σ·T) in the temperature range in which ionic conductivity exists (Figure 4 in Appendices a, b, c) . Based on the experimental values, it was found that the dependence of ln(σ·T) on (1/T), which is characteristic for ionic conductivity in the studied solid solutions, is subject to linear regularity.

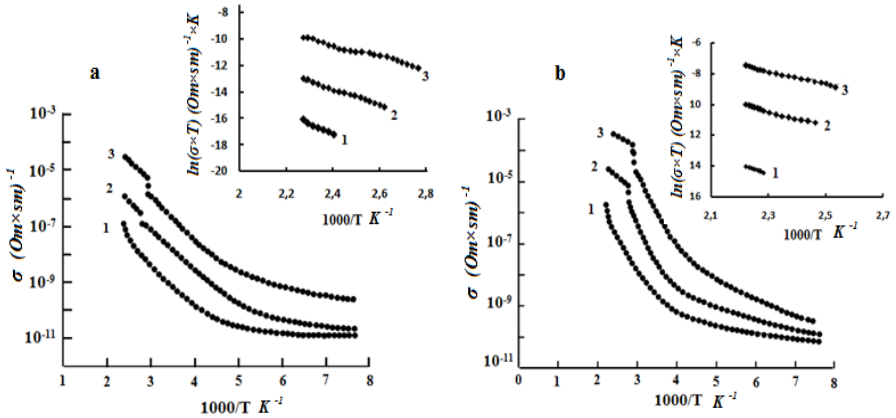

Figure 4. Temperature dependence of the electrical conductivity of the crystal $TlGa_{1-x}In_xSe_{2(1-x)}S_{2x}$ (a-x=0; b-x=0,1); 1-0 MGy, 2-0,25 MGy, 3-0,75 MGy. In the appendices to the figure, the 1000/T dependence of lnσ is given

At temperatures above room temperature, the dramatic change in electrical conductivity observed in solid solutions of the $TlGa_{1-x}In_xSe_{2(1-x)}S_{2x}$ (x=0,6; 0,7; 0,8; 0,9; 1,0) system can be explained by a sharp increase in the number of highly mobile Tl ions, which creates a phase transition to the superion state.

This change occurs as a result of the phase transition of solid solutions of the $TlGa_{1-x}In_xSe_{2(1-x)}S_{2x}$ (0; 0,1; 0,2; 0,3; 0,4; 0,6; 0,7; 0,8; 0,9; 1,0) system, accompanied by irregularity of the Tl sublattice

(melting of the sublattice). Such conductivity is typical for superion conductors. As is known from the literature, along with the exponential increase in electrical conductivity with increasing temperature in substances with superionic conductivity, an exponential increase in dielectric constant is also observed, and at high temperatures its value is many times greater than its value in the low temperature region. Such behavior of the ε(T) dependence in solid solution samples is most likely due to the movement of ions on the defects.

Thus, the high value of the dielectric permittivity of $TlGa_{1-x}In_xSe_{2(1-x)}S_{2x}$**(0; 0,1; 0,2; 0,3; 0,4; 0,6; 0,7; 0,8; 0,9; 1,0)** solid solutions at low frequencies is based on the mechanism of ionic polarization caused by weakly bound thallium ions [7,14, 19]..

In the third chapter of the dissertation the complex impedance and relaxation processes in the frequency range of $25 \div 10^6$ Hs were studied by the method of impedance spectroscopy of $TlGa_{1-x}In_xSe_{2(1-x)}S_{2x}$ crystals and the effect of γ-rays on these processes was studied [12].

Impedance spectroscopy is the most convenient method for studying the electrophysical processes occurring in the metal contacts of ion-conducting materials. In particular, impedance spectroscopy is used to study the dielectric and transport properties of metals, metal oxide or semiconductor electrode / electrolyte interface, to determine the mechanism of electrochemical reactions, to study the properties of porous electrodes, passive surfaces and fuel cells, to evaluate the condition of electrochemical batteries and polymer coatings. In all fields of science, experimental data obtained by impedance spectroscopy are interpreted in terms of "model" in terminology, although the model is considered a reality. The models used to interpret impedance spectroscopy data are analog and physical.

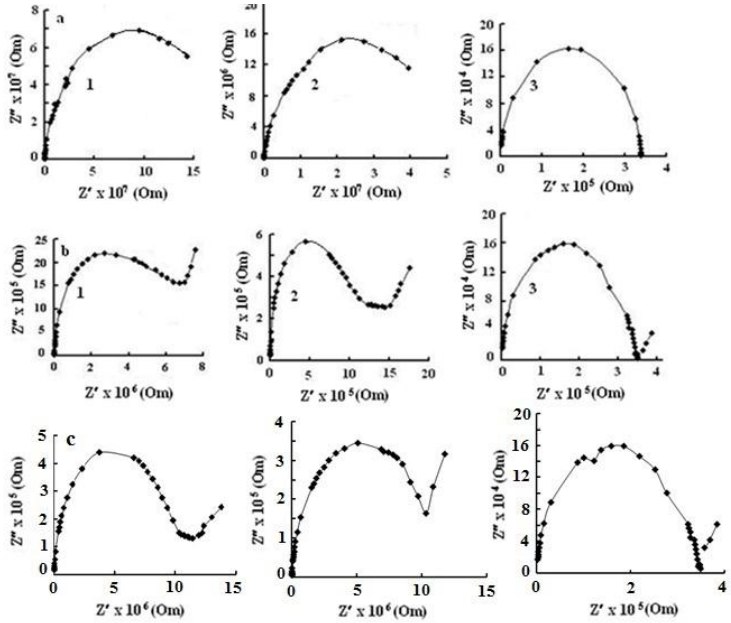

Figure 5. $TlGa_{1-x}In_xSe_{2(1-x)}S_{2x}$solid solution (Z″ - Z′) - diagrams on a complex plane based on the results of measurements Z″ (ω) and Z′ (ω).a–(1) x=0; (2) x=0.2; (3) x=0.4;After irradiation of 0.25 MGy - b–(1) x=0; (2) x=0.2; (3) x=0.4, after 0.75 MGy radiation - c-curve –(1) x=0; (2) x=0.2; (3) x=0.4

Analog models almost always have the form of an electrical equivalent circuit and cannot describe the physicochemical properties of the system, but replicate them schematically. One of the most suitable methods for studying electrochemical and electrophysical processes in ion-transmitting materials is impedance spectroscopy, which is associated with the relatively low cost of the equipment and the relatively high sensitivity of the method. At the same time, there is a problem of interpreting the results obtained. This is due to the complexity of the processes in ionic or mixed electron-ion conducting materials. The development of the theory of impedance spectroscopy, directed to the construction of samples of electrical equivalent circuits, was very difficult. The accumulated experience shows that

the electrical properties of the samples sometimes do not match the resistor-capacitor models. To increase the sensitivity, it is necessary to introduce an inductance or negative capacitance into the equivalent circuit. Thus, there are processes that lead to delays in a phase whose nature is not clear. Another problem is the distribution of electrochemical cores. In the theoretical description of such objects, coordinate and time functions arise, which requires the partial integration of the differential equation. Thus, the assembly of an equivalent circuit that adequately describes the electrical properties of the sample requires serious experimental and theoretical research.

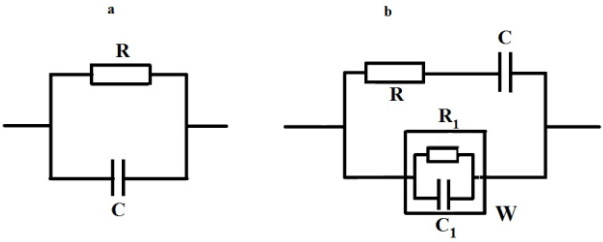

Figure 6. Equivalent circuit. (a-before irradiation, b-after γ radiation). W – Warburg impedance diffusion, R – sample resistance.

The real and imaginary parts of the impedance of $TlGa_{1-x}In_xSe_{2(1-x)}S_{2x}$ solid solution samples irradiated at doses of 0.25 and 0.75 MGy were measured. Based on the experimental results, a description of the complex impedance hodograph is given in Figure 5. For solid solution samples, the arc of a complex plane hodograph describes a curve that is inclined to the real axis near the maximum semicircle at the point of intersection of Z' and Z''.

This form of dependence corresponds to a parallel equivalent substitution scheme (Figure 6 a). In this case, energy transfer is characterized by a single relaxation period. The imaginary part of the impedance shows the maximum at frequencies $f_{(max)}$ corresponding to the condition $C_{eff}R_{eff}\omega_{max} = 1$, where C_{eff} and R_{eff} are the effective parameters of the equivalent circuit, $\omega_{max} = 2\pi f_{max}$is an angular frequency. Figure 5 shows the impedance hodographs for solid solutions of $TlGa_{1-x}In_xSe_{2(1-x)}S_{2x}$ when x = 0, 0.2, 0.4, measurements

were performed before irradiation (curve 6 a), after irradiation 0.25 MGy (curves 6 b).) and 0.75 MGy after irradiation (curves in Figure 5 c). The upper (tip) of the hodograph arc corresponds to the ω_{max} resonance frequency. Z″ are the relaxation times f (max) of the frequencies corresponding to the maximum. Frequencies corresponding to the beginning of frequency dispersion were determined for $TlGa_{1-x}In_xSe_{2(1-x)}S_{2x}$ solid solution samples before and after 0.25 MGy and 0.75 MGy irradiation. Thus, an increase in the frequency $f_{(max)}$ corresponding to the maximum Z″ is observed in the solid solution.

As can be seen, the measurements taken before irradiation have a semicircular shape located in the center of the real axis, which is due to the fact that the charge-carrying process is characterized by a single relaxation period. This type of hodograph is suitable for low-resistance and non-insulating contact homogeneous specimens. The complex plane diagrams obtained from post-irradiation measurements at doses of 0.25 and 0.75 MGy (Z″ - Z′) are semicircular for a parallel RC-chain and are reflected by rays in the low-frequency region of the diagrams (Figure 6 b).

The impedance curves obtained after irradiation of 0.25 MGy and 0.75 MGy show that there are additional effects on the conductivity associated with the diffuse transport of thallium ions in the vicinity of the solid electrolyte and electrode boundary. These rays in the impedance diagram are most likely related to Warburg's diffuse impedance, which means that the sinusoidal signal of a given diffusion carrier cannot reach the diffusion layer boundary in the frequency range. The formation of Warburg's diffuse impedance is considered to be the diffusion of Tl^{+1} ions observed after γ-radiation with the crystal becoming a superion.

It has been found that the relaxation time decreases after the crystals are exposed to radiation. Complex plane diagrams were analyzed using the equivalent circuit substitution method (Z″−Z′). It has been shown that the phase transition of solid solutions of $TlGa_{1-x}In_xSe_{2(1-x)}S_{2x}$to superion occurs after γ-irradiation [20, 24].

The third chapter also presents the results of the study of the frequency dependence of the real and imaginary part of the dielectric

permittivity of $TlGa_{1-x}In_xSe_{2(1-x)}S_{2x}$ solid solution samples irradiated with γ-quanta.

When applying a weakly variable electric field to compounds with irregular structures, the existence of three different charge carrying mechanisms that occur in different temperature and frequency ranges must be taken into account. In delocalized states, the charge carrying occurs at high frequencies. In the case of conduction over localized states, the frequency dependence of the conduction varies by the following law: Re $\sigma(\omega) \sim \omega^s$, where $0.7 < s < 1$. This dependence is realized over a wide frequency range.

This dependence usually occurs at frequencies up to 10^6 Hz. In irregular systems, the charge carrying mechanism is jumping.

This mechanism can be represented as the tunneling of charge carriers through a potential barrier between localized states, based on electron-phonon interactions. In this method, both short-term fixed systems and issues related to the sequential arrangement of nodes in space are considered. In this method, the frequency dependence of the function Ψ (ω) is taken into account, and the share of direct current and high-frequency processes is not taken into account. Different areas of the function Ψ (ω) for three-dimensional systems according to the literature; jumps over infinite clusters, $\Psi(\omega) \sim 1 / \omega$; in the case of a large but finite cluster $\Psi(\omega) \sim \ln\omega$; in the case of a cluster with more than two nodes, Ψ (ω) does not depend on ω; for two-node jumps, Ψ (ω) decreases with increasing ω. Thus, the study of the process of alternating current charge carrying in an irregular condition requires careful analysis of experimental data and selection of the most appropriate model. Impedance spectroscopy is used to measure the dielectric parameters of solids and, as a rule, the expression of the complex dielectric constant $\varepsilon' = \frac{Cd}{\varepsilon_0 S}$ is used.

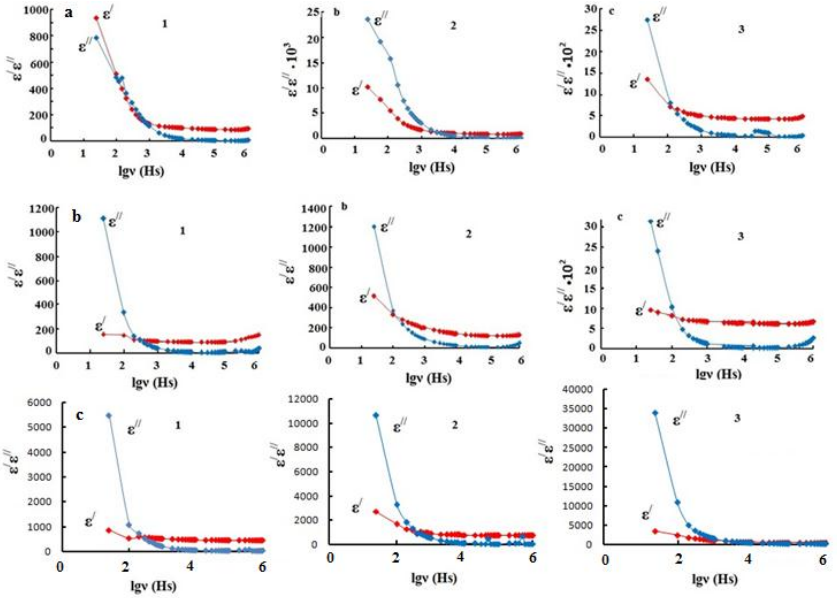

Figure 7. The dependence of the complex dielectric permittivity of solid solutions $TlGa_{1-x}In_xSe_{2(1-x)}S_{2x}$ on the frequency dispersion of real and imaginary parts.

This method allows us to obtain complete information about the thickness of the objects under study and the conductivity properties at the boundary. The real and imaginary parts of the dielectric constant are calculated by the expression $\varepsilon'' = tg\delta\varepsilon'$.

It has been shown that at frequencies increasing from 25 Hz to 10^6 Hs, ε′ decreases weakly and decreases sharply at relatively low frequencies, it has been shown that at high frequencies (f>10^3 Hs) ε′ is weakly dependent on f and at 10^6Hz it has a value of ~ 18.0. At high frequencies, in solid solutions of $TlGa_{1-x}In_xSe_{2(1-x)}S_{2x}$, In high frequency $TlGa_{1-x}In_xSe_{2(1-x)}S_{2x}$ solid solutions, when x = 0, ε′ decreases 10 times, ε′ 2 times for the composition x = 0.1, for x = 0.2, ε′ decreases by 1.5 times. The nature of the frequency variation ε′ and ε″ indicates the presence of a relaxation dispersion of the dielectric constant in solid solutions $TlGa_{1-x}In_xSe_{2(1-x)}S_{2x}$ (figure.7)

At high frequencies, in solid solutions of $TlGa_{1-x}In_xSe_{2(1-x)}S_{2x}$, ε′decreases 10 times when x = 0, ε ′ decreases 2 times for x = 0.1, and ε′decreases 1.5 times for x = 0.2. The nature of the frequency variation ε′ and ε″ indicates the presence of a relaxation dispersion of the dielectric permittivity in $TlGa_{1-x}In_xSe_{2(1-x)}S_{2x}$ solid solutions.

There is a frequency dispersion in the frequency dependence of the imaginary part of the dielectric constant (ε″) of $TlGa_{1-x}In_xSe_{2(1-x)}S_{2x}$ crystals, however, the frequency dependence is weak in samples exposed to gamma radiation before and after radiation. It is known that the activation and relaxation processes in dielectrics are observed to a maximum depending on the frequency ε″ of the imaginary part of the complex dielectric constant. For both primary and irradiated samples, ε decreases with increasing frequency. Such a change is characteristic of an increase in conductivity, because we can write the expression $\varepsilon'' \sim \omega^{-(1-s)}$ taking into account the expression $\varepsilon' \sim \sigma(\omega) / \omega$.

The results of the frequency dependence of the tangent angle of dielectric losses of solid solutions $TlGa_{1-x}In_xSe_{2(1-x)}S_{2x}$are given. For all samples of solid solutions, a maximum in the frequency range $f \sim 10^3$ Hz is observed in the dependence of tgδ(f) and falls to a minimum at a frequency of 10^6 Hs. The value of the frequency dispersion $f_p = 10^3$ Hs and the relaxation time $\tau = 10^{-3}$ was calculated. tgδ(f) indicates the presence and conductivity of relaxation losses in solid solution crystals.

The frequency dependence of $TlGa_{1-x}In_xSe_{2(1-x)}S_{2x}$solid solutions as well as AC-conductivity was given before irradiation, after irradiation at doses of 0.25 and 0.75 MGy. At 10^6 Hz, a sharp increase in the AC-conductivity of solid solutions is observed about 10 times. Gamma radiation has a weak effect on the frequency dependence of conductivity. The presence of solid solutions of $TlGa_{1-x}In_xSe_{2(1-x)}S_{2x}$at 350 K is already in the superion phase, due to the presence of ions in the conduction at this temperature and the irregularity of the system. Thus, under these conditions, additional defects caused by radiation do not affect the frequency dependence of the conduction [15].

It is known that the conductivity in the group of $TlB^3C^6_2$ crystals is transmitted in the presence of localized states near the Fermi level, in the presence of phonons and with the help of variable-length jumps. The characteristic feature of the dependence $\sigma_{ac}(f)$ shows that when $\sigma_{ac}\sim f^{0.6}$ at small frequencies $f \sim 5\cdot 10^5$Hs, this dependence obeys the law $\sigma_{ac}\sim f^{0.8}$. This dependence is due to the localization of states near the Fermi level.

The frequency dispersion of the dielectric permittivity and the relaxor properties of the dielectric loss angle were determined. It has been shown that the charge-carrying mechanism bounces near the Fermi level at 10^5 Hz. The parameters of a given conduction mechanism were evaluated before and after γ radiation. It has been found that the increase in conductivity at T = 350K and 10^6 Hz is due to the transition of the system to superion [9].

In the fourth chapter of the dissertation, the system of $TlGa_{1-x}In_xSe_2$(x=0; 0,1; 0,2; 0,3; 0,7; 0,8; 0,9; 1,0) irradiated with γ-quanta is 100-450K of solid solutions, the results obtained from the study of temperature dependence of electrical conductivity and dielectric permittivity, superion conductivity and impedance spectroscopy in the temperature range and frequency range 25-10^6 Hz are presented.

Based on the results of the study of the temperature dependence of the electrical conductivity of the solid solutions of the system $TlGa_{1-x}In_xSe_2$(x=0; 0,1; 0,2; 0,3; 0,7;0,8; 0,9; 1,0) in the temperature range 100-300 K, the temperature and frequency intervals of the presence of jumping conductivity before and after radiation were determined and the temperature dependences of the Arrhenius coordinates are shown in Figure 8. Depending on this, the temperature range of 180÷260 K is exponential. The dependence of $ln\sigma$ on $T^{-1/4}$ in Mott coordinates in the temperature regions 180<T<260 K is given in Appendices to Figure 8, and it is shown that the experimental points at the determined coordinates converge along a straight line. This allows us to say that in the specified temperature range of non-irradiated and irradiated, charge carrying of

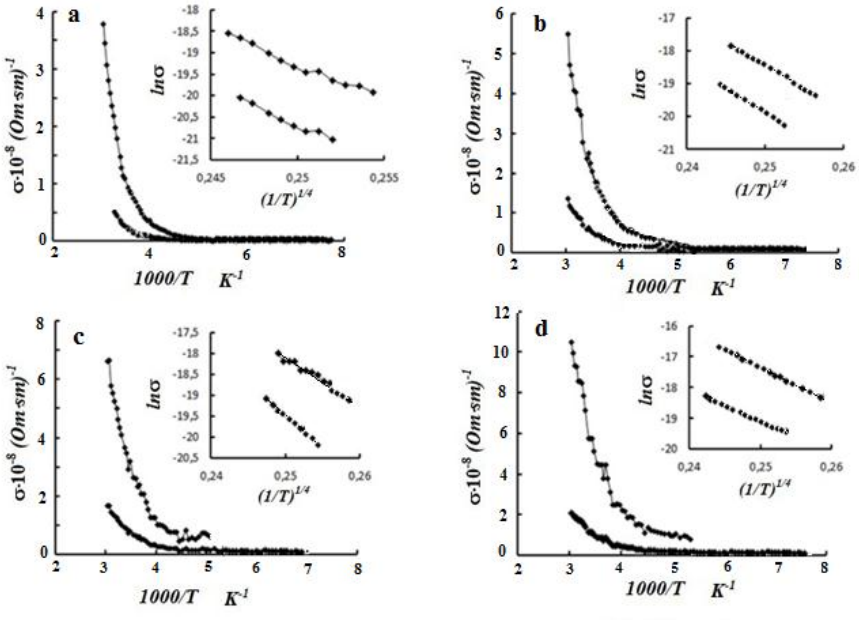

Figure 8. Temperature dependence of the electrical conductivity of solid solutions of the $TlGa_{1-x}In_xSe_2$(1-x=0; 2-x=0,1; 3-x=0,2; 3-x=0,3) system. The appendix on the figure shows the dependence of ln σ on $T^{-1/4}$ in Mott coordinates.

$TlGa_{1-x}In_xSe_2$ (x=0; 0,1; 0,2; 0,3) system in solid solutions is carried out through the jumping conductivity of charge carriers in localized states located in a narrow energy band near the Fermi level.

Temperature dependence of the electrical conductivity of solid solutions of the system $TlGa_{1-x}In_xSe_2$(x=0; 0,1; 0,2; 0,3; 0,7;0,8; 0,9; 1,0) in the temperature range 100-300 K, based on the results of the study, the temperature and frequency intervals of the presence of jumping conductivity were determined before and after irradiation.

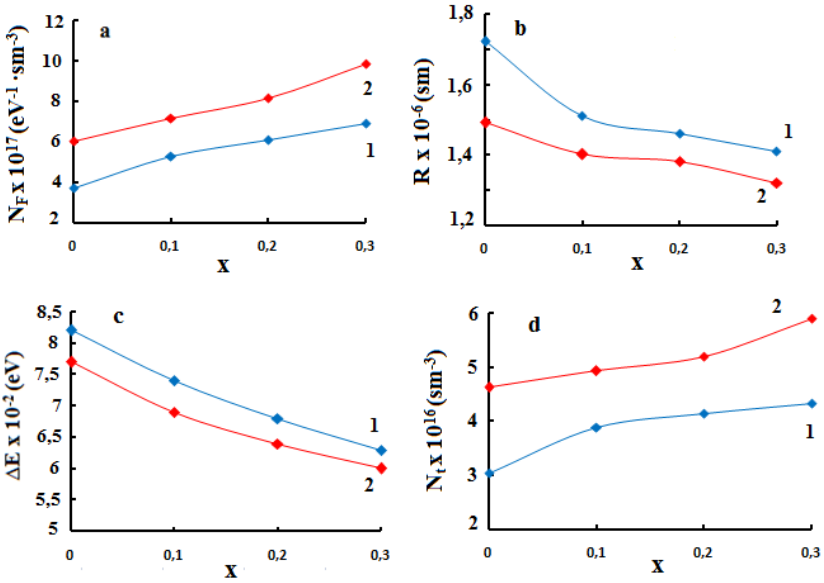

Figure 9. Near the Fermi level of solid solutions of $TlGa_{1-x}In_xSe_2$ (x=0; 0,1; 0,2; 0,3; 0,7;0,8; 0,9; 1,0): a - density of localized cases (N_F), b - energy scattering of localized cases (□E), c - concentration of deep traps (N_t), d - dependence of the length of the jump (R) on the concentration and radiation dose.

Conductivity parameters based on the Mott approximation: Density of localized states near the Fermi level (N_F), concentration of deep traps (N_t), energy difference of localized states near the Fermi level (ΔE) as well as values of average length of carrier jumps (R) calculated, dose and composition dependencies were constructed and are given in Figure 9.

It has been shown that the density of localized states (N_F), near the Fermi level, the concentration of deep traps (N_t) increase depending on the composition of the solid solution and the radiation dose, the energy difference (ΔE) of localized states near the Fermi level, as well as the average length values decrease with the composition of the solid solution and with increasing radiation dose. Additional rea-

sons specific to the jumping nature of conduction have been considered [18].

In the present paragraph of the dissertation work $TlGa_{1-x}In_xSe_2$ (0; 0,1; 0,2; 0,3; 0,4; 0,6; 0,7; 0,8; 0,9; 1,0), ionic conductivity in the temperature range 100-450K and the results of the effect of γ-rays on this conductivity are given.

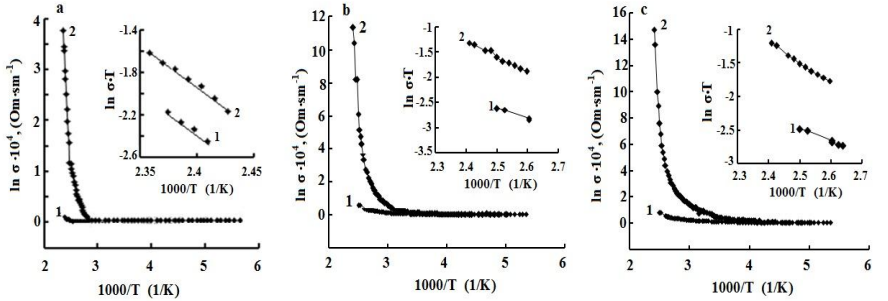

Figure 10 Temperature dependence of the electrical conductivity of solid solutions of the $TlGa_{1-x}In_xSe_2$ system a-x = 0.9; b-x = 0.8; c-x = 0.7. 1-0 MGy, 2-0,75 MGy.

Table 2.

Composition and dose dependence of activation energies of $TlGa_{1-x}In_xSe_2$ (0,1; 0,2; 0,3;) systemic solid solutions.

Composition	**dose**	E_a (eV)
$TlGa_{1-x}In_xSe_2$ (x=0.1)	**0 MGy**	0,15
	0,25 MGy	0,1
$TlGa_{1-x}In_xSe_2$ (x=0.2)	**0 MGy**	0,14
	0,25 MGy	0,08
$TlGa_{1-x}In_xSe_2$ (x=0.3)	**0 MGy**	0,12
	0,25 MGy	0,07

$TlGa_{1-x}In_xSe_2$ (0; 0,1; 0,2; 0,3; 0,4; 0,6; 0,7; 0,8; 0,9; 1,0) in the temperature range of 100-450 K of systemic solid solutions, the temperature dependence of electrical conductivity (σ(T)) was studied before irradiation and after irradiation at a dose of 0.25 MGy (Figure

10) and it was found that the value of conductivity increased several times at a certain critical temperature. Such a characteristic increase in conductivity, as we have noted, indicates that ionic conductivity predominates at temperatures above that critical temperature. As we have noted, such a change in the jumping change in electrical conductivity observed at temperatures above room temperature can be explained by a sharp increase in the number of highly mobile Tl ions, in which a phase transition to the superion occurs.

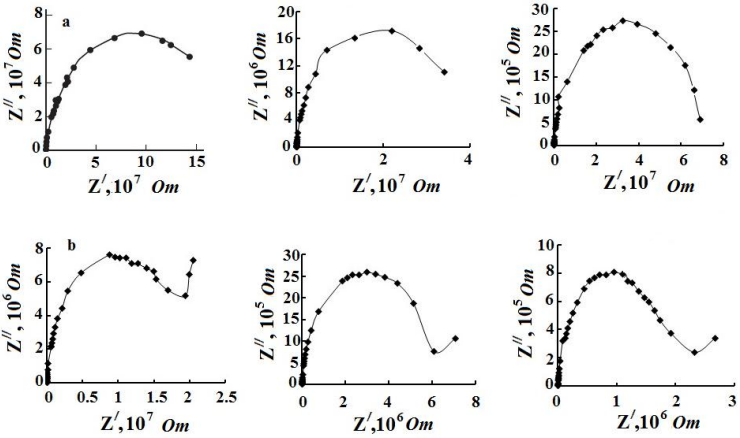

Figure 11. Z″ (Z′) impedance hodograph for solid solutions of $TlGa_{1-x}In_xSe_2$ system. x = 0; 0.2; 0.3. a-0 MGy, b-0,25MGy

Activation energy values of the studied $TlGa_{1-x}In_xSe_2$ (0; 0,1; 0,2; 0,3; 0,4; 0,6; 0,7; 0,8; 0,9; 1,0) systemic solid solutions was calculated based on the expression $\sigma \cdot T = \sigma_0 \cdot \exp(-\Delta E^a / kT)$ and the variation of these values depending on the concentration and dose is given in Table 2.

The complex impedance of solid solutions of the $TlGa_{1-x}In_xSe_2$ system exposed to gamma radiation was also investigated, and the impedance hodographs before and after the radiation dose were shown in Figure 11.

The charge-carrying process before irradiation is characterized by a single relaxation period, but after a dose of 0.25 MGy, the hodograph curves of solid solutions are semicircular for a parallel RC-chain, reflected by rays in the low-frequency region of the diagrams. As we have noted, these rays in the hodograph curves are associated with the diffuse impedance of Warburg [21].The study of the phenomenon of charge carrying in irregular systems in the changing electric field is of practical and fundamental importance. At the same time, the main goal is to determine the mechanism of charge carrying on the basis of known theories [1].

The fourth chapter also identifies the mechanism of charge carrying by studying the nature of electrical conductivity in solid solutions of TlGa1-xInxSe2 over a wide range of temperatures (180, 230, 300K) and frequency (25-10^6Hz).There is a sharp decrease in the $Z'(f)$ and $Z''(f)$ curves in the studied frequency range, but a weakening of the dependence is observed with a further increase in the frequency in the studied spectra. This indicates the presence of dispersion in the impedance spectra.

The impedance hodograph curves of $TlGa_{1-x}In_xSe_2$ solid solutions at different temperatures are given in Figures 12 and 13. The obtained hodograph curves can be divided into two parts, indicating the presence of two relaxation mechanisms. The high frequency part of the $Z''(Z')$ dependence is related to the relaxation process in the vast majority of the solid solutions studied. The relaxation mechanism in the low-frequency part of the impedance hodograph of solid solutions is related to the diffusion mechanism associated with the presence of a concentration gradient of carriers in the surface region. Thus, the mechanism of energy loss in solid solution samples is related to conductivity and consists of losses associated with relaxation polarization. As can be seen from Figures 12 and 13, the arc of the complex hodograph for the composition of the solid solution at high frequencies depicts curves close to a semicircle with centers at the real axis, and the charge-carrying process is characterized by a relaxation period. This type of hodograph is suitable for homogeneous specimens with low resistance and no insulating contact.

In this case, the equation scheme using the impedance components of the electrical circuit for the impedance coefficients 0, 0.2, and 0.3 of the solid solutions of $TlGa_{1-x}In_xSe_2$is described.

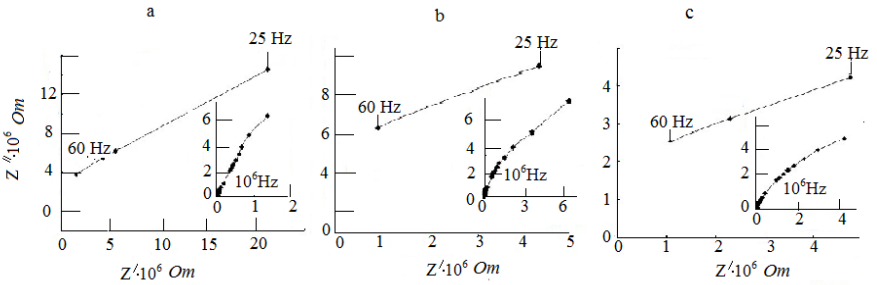

Figure 12. Hodograph curves in low-frequency and high-frequency parts of solid solution samples $TlGa_{1-x}In_xSe_2$. Figure a, b, c respectively x = 0; 0.2 and 0.3. T = 300 K.

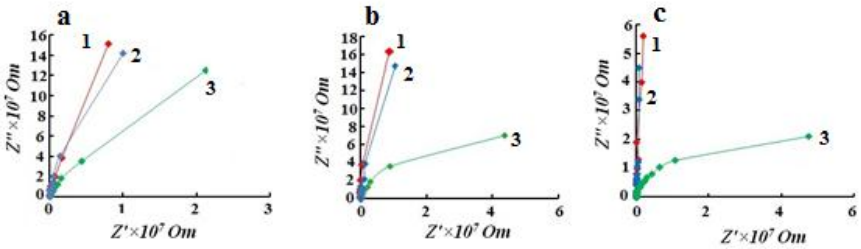

Figure 13. Impedance hodograph of solid solutions $TlGa_{1-x}In_xSe_2$. Figure a, b, c respectively x = 0; 0.2 and 0.3. Curves 1, 2 and 3 are 180, 230 and 300 K, respectively.

Such an equivalent circuit for the high frequencies section is shown in Figure 6. The equivalent circuit in Figure 6 b corresponds to the low frequency range. At a temperature of 300 K, the rays observed in the low-frequency region on the impedance hodograph curves are associated with solid electrolyte and diffuse ion transport near the surface.

The frequency dependence of the real and imaginary parts of the complex dielectric constant of $TlGa_{1-x}In_xSe_2$ solid solutions at temperatures of 180, 230 and 300K is shown. As the frequency of electric field measurements increases, the prices of complex dielectric components decrease, which indicates the presence of dispersion.

Non-irradiated and irradiated at a dose of 0.25 MGy $TlGa_{1-x}In_xSe_2$ x=0; 0.2; 0.3, the frequency dependence of the real and imaginary part of the dielectric permittivity of solid solutions was studied. Observation of the decrease in the values of the complex impedance components with the increase of the measuring frequency of the electric field reveals the dispersion properties. It was found that with increasing frequency from 10 to 10^6 Hs, ε′ decreases weakly and decreases sharply at relatively low frequencies, at high frequencies (f>10^3 Hs) ε′ is weakly dependent on f, and at 10^6 Hz it receives a value of ~ 18.0 shown. For $TlGa_{1-x}In_xSe_2$ solid solution crystals, these values of the high-frequency dielectric constant are the same as the values of the optical dielectric constant ε ′. The nature of the frequency dispersion of samples exposed to gamma radiation at a dose of 0.25 MGy varies slightly. At high frequencies, $TlGa_{1-x}In_xSe_2$ decreases 10 times in solid solutions when x = 0, ε ′, for x = 0.2, ε ′ decreases by 2 times, and for x = 0.3, ε ′ decreases by 4 times. The nature of the frequency variation ε ′ and ε ′ ′ indicates the presence of a relaxation dispersion of the dielectric constant in solid solutions $TlGa_{1-x}In_xSe_2$ [23].

Non-irradiated and irradiated solid solutions of $TlGa_{1-x}In_xSe_2$ at a dose of 0.25 MGy, at a temperature of T = 300 K, the frequency dependence of AC conduction is shown in Figure 14. As can be seen from the figures, a sharp increase in the AC conductivity of the solid solution at about 10 times is observed at frequency 10^6. As can be seen from the figures, the effect of radiation on the frequency dependence of electrical conductivity is practically unnoticed. This is due to the fact that the studied solid solutions are located in the superion space at a temperature of 300 K and a frequency of 10^6, at this temperature and at this frequency the conductivity is mainly ionized and the system is disordered.

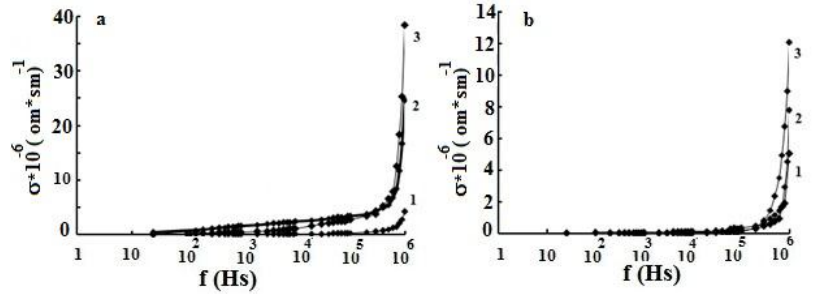

Figure 14. AC-conductivity of solid solutions $TlGa_{1-x}In_xSe_2$ (x=0.1)in the temperature range T = 300K. Fig. a-0 MGy curve 1 – x = 0; 2 – x = 0.2; 3 – x = 0.3: b – 0.25 MGy curve 1 – x = 0; 2 – x = 0.2; 3 – x = 0.3.

Thus, under these conditions, additional defects do not affect the frequency dependence of electrical conductivity when exposed to radiation.

For all the studied components, two features are observed in the frequency regions f = 10^2 and 10^5 - 10^6 Hs. Thus, the charge carrying mechanism in the variable field will be determined by the following factors:

a- presence of Ga and In tran transmission irregularities and point defects in the studied solid solutions of $TlGa_{1-x}In_xSe_2$ substitution;

b - the presence of frequency dispersion - affects the charge carrying mechanism;

c - the mechanism of electrical conductivity, the presence of a temperature factor that can be transformed from the delocalized states free-phonons in the presence of phonons into a jumped conductivity in the presence of phonons in the localized states;

d - the presence of blocking contacts that affect the nature of the electrical conduction at high temperatures, ie when the ionic conductivity in the electrical conductivity begins to play an important

role. It has been found that in weakly variable electric fields, it is carried out by a jumping mechanism of carriers on localized states near the Fermi level. Quantitative evaluation of the parameters was carried out within the framework of the effective mean theory and Mott's approximation.

The fifth chapter of the dissertation presents the results of the study of the electrical and dielectric properties of $TlInS_2$ crystals doped with vanadium atoms and Van der Waals surfaces by atomic force microscopy and the effect of γ-rays on these properties.

The impurity of $TlInS_2$ crystal with some mixtures leads to an increase in dielectric sensitivity in the irregular phase region. The cause of relaxation was found to be the formation of nanoscale polar domains, which caused the regular phase to precede the dipole and segnetoelectric glasses. The impurity atoms that lead to the relaxation state, in turn, form retention levels in the forbidden zone of the semiconductor-segnetoelectric $TlInS_2$ crystal. The charge carriers that fill these levels are phase-limited, and as a result, in this case, the conduction is carried out through a tunnel in the potential wall. When the charge-carrying process was observed in $TlInS_2$ crystals doped with V atoms, a temperature-independent jumping conductivity in the dimensionless phase region was also determined.

The temperature dependence of the dielectric permittivity ε(T) of the $TlInS_2$ crystal detected with vanadium was studied. In the $TlInS_2$<V> crystal, the variation of the diffuse maxima of the dependence ε(T) is 5K as the frequency increases from 1 kHz to 1 MHz. As we assume, the condition for the formation of a relaxation state in the $TlInS_2$<V> crystal is the adaptation of the phase transition temperature and the thermo-filling of the local centers to the temperature region. The properties of relaxations can also be significantly changed by applying a small amount of the mixture, which affects the energy state of the compounds. In this case, the change in the maximum temperature of the dielectric permittivity can reach several degrees. An important feature of segnetoelectrics with diffuse phase transitions is that their dielectric constant changes above the temperature T_m not by the Curie-Weiss law, but by the law $\varepsilon^{-1/2} = A + B(T-$

T_0). The broadcast nature of the ε(T) dependence is a necessary condition for a relaxed state

The most likely mechanism for the formation of radiation defects in the vanadium-detected $TlInS_2$ compound is the multilayer ionization of the mixed vanadium atom. The resulting defect increases the energy levels of the crystal in the restricted zone, and the thermo-filling of these levels occurs at a relatively lower temperature than in a non-radiated compound. That is, the area where the segnetoelectric glass exists is expanding.

The results of the study of the temperature dependence of the electrical conductivity σ(T) and dielectric constant in a given electric field in the frequency range 1kHs-1MHs of the crystal $TlInS_2$<V> are presented. The dependence of σ(T) on the temperature range $T_d - T_f$ is described by Mott's law and corresponds to the mechanism of jumping conduction. It is in this temperature range that $TlInS_2$<V> is in the form of segneto-glass. In the temperature range below T_f =170K, the conductivity is practically independent of temperature. The results of the study of the frequency dependence of the electrical conductivity of the crystal $TlInS_2$<V> at temperature T=200K are given. In the frequency range 10^3-10^6 Hz, the electrical conductivity varies by the law of $\omega^{0.8}$. This shows the jumping mechanism of the carriers due to the cases localized near the Fermi level. Under the influence of an alternating electric field, the parameters were calculated within the Mott approximation of the $TlInS_2$<V> crystal. It is shown that the jumping conduction takes place below the Burns (T_d) temperature. There is thermoactivated conduction up to the Fogel-Fulcher temperature (T_f), and below T_f there is an inactive jumping conduction [3, 4, 11].

In the fifth chapter of the dissertation, determination of the basic physical laws of plastic deformation on the surfaces of $TlInS_2$ <0.1%V>crystals and solid solutions of $TlGa_{1-x}In_xSe_2$ (x=0; 0.1; 0,2)detected by layered $TlInS_2$ and vanadium (V) and the general kinetic process that affects the structure of their surfaces at the nanoscale is described.

The creation and study of nanostructures with controlled dimensions and properties is one of the most important technological challenges. The main reason for this is due to the revolutionary changes in the field of nanoelectronics, materials science and the scope of this problem. Reducing the size of nanostructured elements plays a key role in the study of many properties that play a key role in the development of microelectronic devices.

This chapter examines the basic physical laws of plastic deformation on the surfaces of irradiated layered crystals and the general kinetics that affect their surface structure at the nanoscale.

The probe method allows to determine the mechanisms and conditions of their formation and development, which clearly describe the form of the structural structure of nanoscales. Nanoscale structural elements change surface properties and exhibit low-dimensional quantum effects that cause changes in many electrical, physical, and mechanical parameters of the surface.

Layered crystals are related to different types in terms of strength. Strong covalent or ion-covalent bonds and weak molecular Van der Waals bonds perpendicular to the layer occur along the fission plane. Layered semiconductor crystals have anisotropic properties with electrical, mechanical, optical and other properties. Due to the above properties, layered-chain semiconductor crystals $TlGaSe_2$, $TlInSe_2$ and solid solutions based on them are relevant for research.

In terms of the regularity of the atom, the crystal surfaces do not collapse easily. The resulting surface tension creates an unstable state in the surface layer of the atoms. The relaxation of the outer atomic layer leads to the displacement of the atomic layer following the surface. In particular, studies of alkali metal chalcogenide crystals show that the crystal structure approaches a volume at a depth of at least five layers, and for some crystals this depth can exceed tens of atomic layers. The most suitable objects for studying processes on clean surfaces are crystals with perfect layers, such as mica or layered crystals.

In this regard, the study of the formation of nanoscale gaps on the surface of van der Waals of layered crystals and solid solutions

formed between them is of great interest. High durability, small surface roughness and the absence of broken bonds allow to study the fracture morphology of the surface of solid solutions of $TlGaSe_2$-$TlInSe_2$ by atomic force microscopy (AFM) at air and room temperature.

The problem of determining the basic physical regularity on the surfaces of $TlInS_2$ <0.1%V>crystals of deformation detected by layered $TlInS_2$ and vanadium and the general kinetic process that affects the structure of their surfaces at the nanoscale. The following examines the regularity of the properties of the evolution and formation of folded and dislocated structures in the surface layers, and the effect of their kinetics on the surface structures at different stages. Geometric dimensions and profiles of structural formations in the VDV surface layer of TlInS2 and TlInS2 <0.1% V> layered crystals were determined by atomic force microscopy. Due to the nature of the formation of visser and folded elements, it is observed that the deformation of the surface layers is responsible for both the initial and final stages of deformation, which go hand in hand with the natural domestic oxidation process. The factors corresponding to the characteristics of the plastic flow were analyzed. In this regard, the study of the formation of nano-sized gaps on the surface of the Van der Vaals of the layered $TlInS_2$ crystal is of interest. It has been determined that plastic deformation of the Van der Waals surface of the $TlInS_2$ crystal results in various linear defects and nanoscale bubbles.

The aim of this work is to study the morphology at the level of $TlInS_2$and $TlInS_2$<0.1% V>obtained by fragmentation using the atomic force-microscope method at room temperature. For atomic force-microscopy studies, the Van der Waals surface of the sample, several upper layers of the monocrystal, were removed from the air with adhesive tape. The length and measurement of the subsequent structure of the Van der Waals surface to be examined on the scanning table of the atomic force microscope did not exceed 2-3 minutes. The scan area was determined by a video camera with a magnification of one hundred mounted on the microscope interface, ~ 5x5 mkm^2. From the images of the atomic force-microscope of the

study, the roughed mean-square value of the base of a pure TlInS2 crystal was ~ 0.053 nm, ie this surface can be considered smooth-atomic. Molecules adsorbed on the surface form nanoscale clusters arranged in a regular pattern on the surface. Research interest in this field is related to the acquisition of various nanostructures up to 100 nm.

T = 300K was obtained in the atmosphere, $TlInS_2$ and $TlInS_2$ <0.1%V>on the 3D scale in the form of an atomic force-microscope, separate viscous nanoelements were observed, which took the form of cones. 2D images of $TlInS_2$ and $TlInS_2$ <0.1%V>crystals were obtained.

The maximum difference in height is in the direction of the selected surface (0001), 40nm, and takes the form of a shrinkage surface, the process of self-organization of the surface of the transverse $TlInS_2$ crystal. This leads to mechanical resistance of the bonding forces between the layers and anisotropy of the anarmony. It was found that self-arranged, folded structures have fractal profiles with a difference of several nanometers in height.

In the upper layer of the $TlInS_2$ crystal, nano-sized bubbles with a polygonal shape are observed in the field (001). The formation of nanoscale bubbles occurs as a result of the rupture of covalent bonds. This defect occurs during the injection of vanadium atoms. $TlInS_2$ <0.1%V>were mainly V_2S_3clusters on the surface. Nanoscale bubbles in the polygonal position in the upper layer of $TlInS_2$ <0.1%V>are shown in Figure 15.

Nano-sized folders are located mainly along the scanning line. Based on this, the needle-shaped form of nano-sized folders of the $TlInS_2$ crystal, exposed to vanadium, and the use of cathode emitters for semiconductor field devices are particularly attractive. At the time of the formation of nanoscale bubbles, after the covalent bond in the upper layer is broken, $TlInS_2$ atoms accumulate in droplets and are poured into the interlayer. They were bound by the molecular forces of the next lower layer of the surface. The formation of such a small surface of the $TlInS_2$ crystal has been observed from the literature.

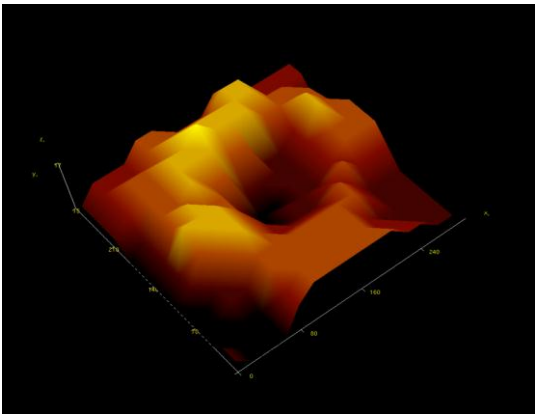

Fig.15. $TlInS_2$ <0.1%V>. a nanoscale bubble in a polygonal position in the upper layer.

The vanadium atoms that fall into the nanoscale bubbles repeatedly collide with each other, reflected from the walls of the nanoscale bubbles. As a result of this effect, the saturation rate of nanosized bubbles increases, the ability of molecules to dissociate increases, and leads to the formation of critical embryos. Rapid formation, growth and coalescence of a large number of embryos occur during the catalysis of the metal. The growth of conical clusters occurs due to vanadium atoms entering along the surface of the $TlInS_2$ crystal (001).

It was shown that the profilograms and histograms of the layered solid solutions studied by the Atomic Force Microscope method were measured. The reason for the spontaneous faceting of a surface is that the ratio of the free energy of the surface to the crystallographic axis depends on the direction of this surface. If a smooth surface has a large specific surface energy, it spontaneously becomes a "trap and hollow" structure. This reduces the total free energy of the surface, despite the increase in total area. The resulting roughed structure is determined by the minimum free surface energy [6]. The fifth chapter of the dissertation also presents the results of the study of surface

processes of solid solutions of $TlGa_{1-x}In_xSe_2$ (x=0;0.1;0,2) irradiated with γ-quanta under an atomic force microscope.By the anisotropy of the chemical compounds in and out of the layer of solid solutions of $TlGaSe_2$-$TlInSe_2$, it is possible to obtain a low-density surface condition of a smooth surface.

Because little is known about the surface properties of the samples studied, scanning began at ~ 14 mкm2. Based on the scan results, the optimal scanning speed was taken. Then the scan area was changed to the smallest side. According to the scan results, the scan parameters were found. These parameters initially include the choice of the oscillation frequency of the probe and determine the minimum distance of the measured surface from the probe. Scanning speed (within 2-3 mkm/s), scanning step and feedback increase were also taken. The studies were performed at room temperature.

The 2D image of the surface by the scanning method is shown in the direction of division and the drawn profilogram (Figures 16 and 17 a and b). The images show that the profile height varies between 4-7 nm, but the lateral dimensions can reach 10 nm. Scanning of part of the surface of solid solutions of $TlGa_{1-x}In_xSe_2$ (x=0; 0,1; 0,2) by order of tens of microns did not change the structure of the surface and its morphology. The absence of non-roughed structures can be explained by the directional movement of atoms along the surface, which leads to the development of semiconductor wave and step structures on the surface.

In the upper layer of solid solutions of $TlGa_{1-x}In_xSe_2$ (x=0; 0,1; 0,2), polygon-shaped clusters of polygonal shape are observed in the area (001). The formation of nanoscale clusters occurs as a result of the breaking of covalent bonds in the upper layer of layered crystals. These defects occur during radiation exposure. Formation of nanoclusters occurs as a result of breaking of covalent bonds in layers in solid solutions of $TlGa_{1-x}In_xSe_2$ (x=0; 0,1; 0,2).

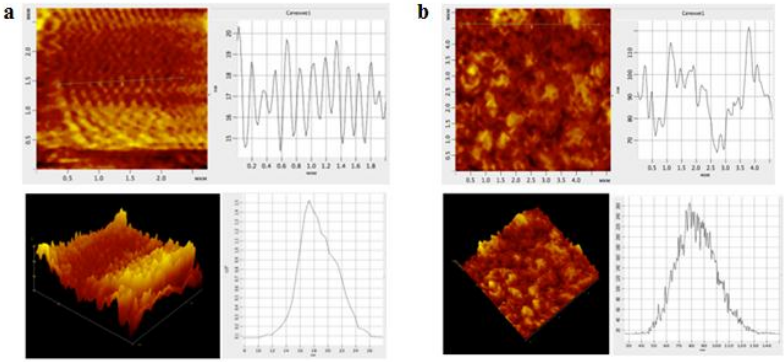

Figure 16. Profilogram of $TlGaSe_2$ crystal, b-3D, histogram. a-0 MGy, b-0.25 Mgy

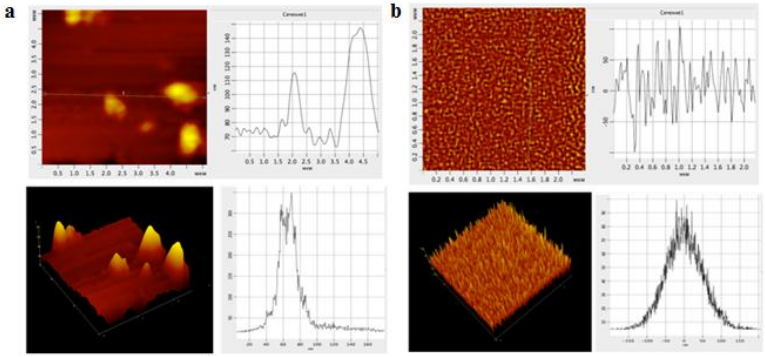

Figure 17. $TlGaSe_2$-90%-$TlInS_2$-10%, profilogram, 3D, histogram. a- 0 MGy, b-0.25 MGy.

When nanoscale clusters are formed, after the covalent bond in the upper layer is broken, the In atoms accumulate in droplets and pour into the layer.

The effects of radiation increase the saturation of nanoscale clusters, increase the ability of molecules to dissociate, and lead to the formation of critical embryos. The rapid formation, growth, and coalescence of a large number of nanoscale clusters occur during the catalysis of the metal. Radiation causes the growth of conical clusters. The presence of a force acting perpendicular to the layers of sol-

id solutions of $TlGa_{1-x}In_xSe_2$ (x=0; 0,1; 0,2) and plastic deformation is carried out by friction of dislocations. In our experiment, the decomposition of $TlGa_{1-x}In_xSe_2$ (x=0; 0,1; 0,2) solid solutions under the influence of deformation causes bending in the form of concentrated loading. Maximum deformation occurs on the lower surface of the studied solid solutions and exists with increasing external loading due to changes in the elastic surfaces.

The height of nano-sized bubbles reaches 7-14 nm. Subsequent scans increased the density of nanoscale clusters without increasing the height dimension. Structural surface defects are formed in the base area (001). The low energy generation of vacancies is due to the predominance of radiation defects in this area. The plastic flow occurring in the conical pyramidal friction field of layered-chain crystals causes the agitation of other layers corresponding to the distribution of solid solutions $TlGa_{1-x}In_xSe_2$ (x=0; 0,1; 0,2) up to 6 nm and covers ~ 7 ÷ 8 layers. The presence of horizontal layer cracks in the conical walls of such nano-sized bubbles does not allow the formation and rapid formation of nano-sized bubbles.

X-ray diffractometric reflexes were studied due to the determination of the composition of nanoobjects formed on the surface of solid solutions of $TlGa_{1-x}In_xSe_2$ (x=0; 0,1; 0,2). Based on the nanoparticles described in figure 16 and 17 a and b, it was determined that these nanoobjects were most likely formed by the In elements (after exposure to radiation). Objects on the surface of solid solutions $TlGa_{1-x}In_xSe_2$(x=0; 0,1; 0,2) are mainly due to clusters In.

Nanoscale clusters are located mainly along the scanning line. Especially attractive is the use of solid solutions of pure $TlGa_{1-x}In_xSe_2$ (x=0; 0,1; 0,2) without the influence of radiation in the form of needles in nanoscale clusters, cathode emitters for semiconductor field devices.The morphology of solid solutions of $TlGa_{1-x}In_xSe_2$ (x=0; 0,1; 0,2) on the Van der Waals surface was studied. Nanoparticles are observed with the placement of a small surface density on the Van der Waals surface of solid solutions of $TlGa_{1-x}In_xSe_2$ (x=0; 0,1; 0,2)obtained by the flaking method. Such AFM images are characteristic of a large number of layered crystals. Differences within

the interatomic bonds and between the layers cause anisotropy of the physical properties of the layered crystal. Based on the anisotropy of the chemical bonds between and within the layers in the studied solid solutions, it is possible to obtain a smooth atomic surface by the method of flaking [8].

In the image of an atomic force microscope, separate nanoscale clusters with a pyramidal shape can be observed. Description of the atomic force microscope must take into account the interaction between the layered crystal surface and the probe and the effect of other atmospheric influences on the sample. Theroughedsystem of defects and adsorbed particles on the surface of the Van der Waals results in the formation of a surface with a minimum energy of balance, forming itself. Such processes form roughedstructures on the surface of Van der Waals.

It should be assumed that the layered-chain crystal is self-organizing as a result of cooperative dislocation processes in the base and pyramidal crystallographic areas in the upper parts of the roughedsurface. At the maximum, characterized by minimum amplitude values and large period values, the simple roughedsurface with periodic variation was observed. They are responsible for the formation of their own defects and the presence of oxide nanoscale clusters in the depths of the layered crystal.

In this multifaceted form, surface defects (clusters of point defects) on the base surface are detected by atomic force microscopy.

The mechanical properties of crystals are affected by the following factors: the type of crystal lattice, the presence of impurities, the effect of radiation, the orientation of the crystal according to the deformation force, the temperature and speed of deformation, size, shape and surface condition of the crystal, etc.

The shape, lateral size and distribution of nano-sized bubbles in the upper layer of the Van der Waals surface on the surface of solid solutions of $TlGa_{1-x}In_xSe_2$(x=0; 0,1; 0,2) depends on the conditions of technological deposition of the material, the type of intercalant clusters (electronegativity, atomic size), dimensions, surface tension distribution. Modern nanoelectronics requires the creation of new-generation devices, light and thermoelectric energy converters. To

achieve this, they convert light energy into electrical energy and convert electrical energy into polarized light based on strong anisotropic semiconductor compounds.

The sixth chapter of the dissertation presents the results of the study of the optical properties of solid solutions of $TlGa_{1-x}In_xSe_{2(1-x)}S_{2x}$and $TlGa_{1-x}In_xSe_2$ systems irradiated at doses of 0; 0.01; 0.02; 0.05 and 0.25 MGy in the fundamental absorption region.

Crystals of $TlInS_2$ and $TlGaSe_2$ (and their solid solutions) are attractive in the acquisition of optoelectronic devices due to their high photosensitivity in the visible region of the spectrum, wide spectral range of transparency, segnetoelectric and pyroelectric properties. Due to their high mass density, thallium-containing chalcogenides are promising materials for radiation detection. Layered chalcogenide compounds can be prepared in complex crystalline structures used in photoreconductivity where the forbidden zone is controlled over a wide energy range (0.6-2.4 eV).

Many optical spectroscopies have been performed perpendicular to the plane of the layer under normal light. It was found that optical transitions predominated above the edge of the inverse forbidden zone. Different simplified approaches were used to derive the values of the forbidden zone in the range of E^d_g=2.08−2.23 eV of the straight forbidden zone and E^i_g=1.83−2.13 eV of the inverse forbidden zone. The change in the energy of the forbidden zone is due to the presence of different polytypes of the $TlGaSe_2$ crystal.

The absorption coefficient is determined as follows using the literature data

$$\alpha = \frac{1}{d}\ln\left(\frac{(1-R)^2 + \left[(1-R)^4 + 4R^2T^2\right]^{\frac{1}{2}}}{2T}\right)$$

Here, R is the reflection (0,2605 [22]), α is the optical absorption coefficient, and d is the thickness of the sample.

Reflection measurements were carried out on samples taken from natural layers by fragmentation, and the thickness of the samples was taken as αd>>1. The thickness of the samples used in the experiment was around d≈300 μm.

As mentioned above, the fundamental absorption coefficient in most semiconductors is determined by the following regularity:

$$\alpha\hbar\omega = B(\hbar\omega - E_g)^n$$

where $\alpha\hbar\omega$ is the absorption coefficient, $\omega = 2\pi\nu$ -is the angular frequency, n is constant, and the n index can be 1/2, 3/2, 2 and 3, the nature of the dependence depends on the absorption spectrum of the electron transition. In the high-energy region of the spectrum, n = 1/2 indicates the allowed straight transition, n = 3/2 shows the forbidden straight transition, in the lower energy part of the spectrum, n = 2 shows the allowed cross transition, n = 3 indicates the forbidden cross transition .

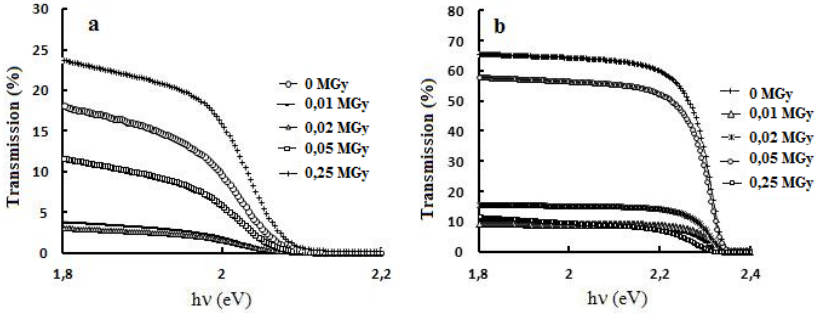

Figure 18. Emission spectra of $TlGaSe_2$ (a) and $TlInS_2$ (b) crystals at T = 300 K.

In this chapter, 0, 0.01; 0.02; 0.05; 0.25 Mgy, the results of the study of the emission spectra of $TlGa_{1-x}In_xSe_{2(1-x)}S_{2x}$ and $TlGa_{1-x}In_xSe_2$ systemic solid solutions at room temperature irradiated in the dose range of 0.25 MGy are given (fig.18). The purpose of this study was to obtain new information about the optical properties of the solid solutions studied after γ-irradiation. The main purpose of the research is to study the optical properties in the fundamental absorption region of solid solutions of the system $TlGa_{1-x}In_xSe_{2(1-x)}S_{2x}$ and $TlGa_{1-x}In_xSe_2$ during isomorphic, as well as cation-anion displacement.

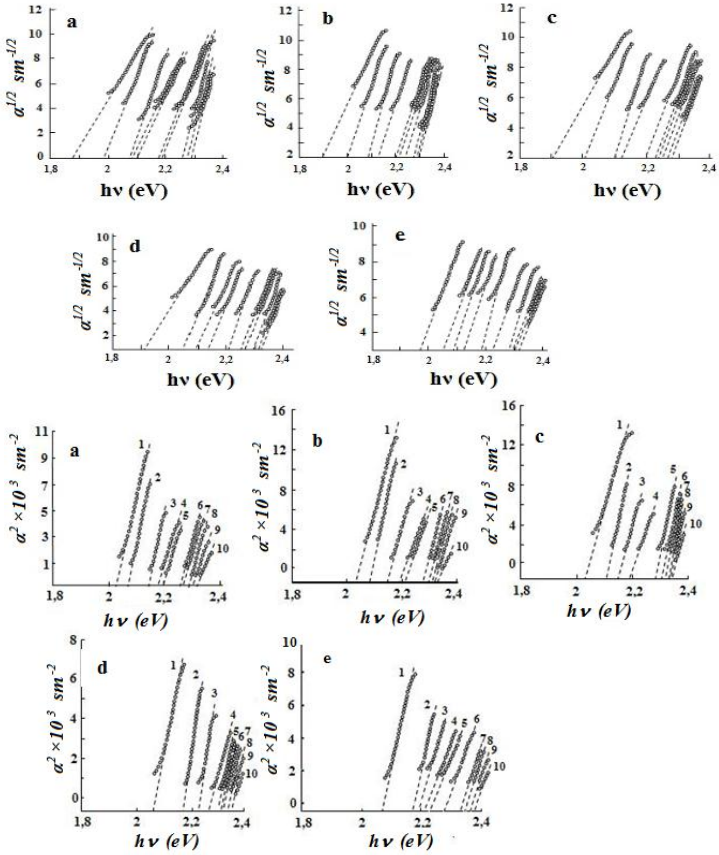

Figure 19. Dependence of the absorption spectrum of solid solutions of $TlGa_{1-x}In_xSe_{2(1-x)}S_{2x}$(x= 0; 0.1; 0.2; 0.3; 0.4; 0.6; 0.7; 0.8; 0.9; 1.0) system at room temperature on the energy of the photon (a- 0 MGy, b- 0.01 MGy, c- 0.02 MGy, d- 0.05 MGy, f- 0.25 MGy).

$TlGa_{1-x}In_xSe_{2(1-x)}S_{2x}$ (x = 0; 0.1; 0.2; 0.3; 0.4; 0.6; 0.7; 0.8; 0.9; 1.0) The absorption spectra of samples of solid solutions of the system exposed to 0 MGy, 0.01 MGy, 0.02 MGy, 0.05 MGy and 0.25 MGy radiation at room temperature were studied. According to the experimental results, the absorption coefficient $TlGa_{1-x}In_xSe_{2(1-x)}S_{2x}$

(x = 0.6; 0.7; 0.8; 0.9; 1.0) at a temperature of 300K is 5 cm^{-1} and 110 cm^{-1}, respectively, in solid solutions.

For samples $TlGa_{1-x}In_xSe_{2(1-x)}S_{2x}$ and $TlGa_{1-x}In_xSe_2$, the optical absorption energy transition to the straight and across of the forbidden zone is determined using the dependencies ($\alpha^{1/2}$-$\hbar\omega$) and (α^2-$\hbar\omega$), respectively, it is obtained from the extrapolation of the lower fragmented part of the straight line to the values $\alpha^2=0$ and $\alpha^{1/2}=0$. In Figures 19 and 20, before irradiation at room temperature and exposed to 0.01 MGy, 0.02 MGy, 0.05 MGy and 0.25 MGy radiation, the spectral dependence of the permissible optical transitions on the photon energy of the straight and across of the samples of solid solutions $TlGa_{1-x}In_xSe_{2(1-x)}S_{2x}$(x= 0; 0,1; 0,2; 0,3; 0,4; 0,6; 0,7; 0,8; 0,9; 1,0) is given. In the 0-25 Mrad dose range, variations were observed between 1.90–1.98 eV for $TlGaSe_2$ and 2.32–2.35 eV and 2.27–2.32 eV for $TlInS_2$ crystals.

Figure 21 shows the concentration-dependent curve of the width of the straight and cross forbidden band of samples of solid solutions $TlGa_{1-x}In_xSe_{2(1-x)}S_{2x}$ (x= 0; 0,1; 0,2; 0,3; 0,4; 0,6; 0,7; 0,8; 0,9; 1,0) exposed to 0 MGy, 0.01 MGy, 0.02 MGy, 0.05 MGy and 0.25 MGy radiation. As can be seen from the figure, the $TlGa_{1-x}In_xSe_{2(1-x)}S_{2x}$ system increases the width of the forbidden band with increasing concentration and radiation dose in solid solutions.

As mentioned, this chapter also presents the results of the study of optical properties in the fundamental absorption region of $TlGa_{1-x}In_xSe_2$ (x= 0; 0,1; 0,2; 0,3; 0,7; 0,8; 0,9; 1,0) systemic solid solutions. According to the experimental results, the absorption coefficient of $TlGa_{1-x}In_xSe_2$ (x= 0,6; 0,7; 0,8; 0,9; 1,0) solid solutions in samples exposed to 0 Mrad and 5 Mrad at a temperature of 300K is 5 cm^{-1} and 140 cm^{-1}, 5 Mrad in non-irradiated samples, respectively, and 10 cm^{-1} və 70 cm^{-1} in samples irradiated at a dose of 5 Mrad.The dependence of the permissible straight and cross optical spectra on the photon energy of the samples of solid solutions $TlGa_{1-x}In_xSe_2$ (x= 0; 0,1; 0,2; 0,3 0,7; 0,8; 0,9; 1,0) exposed to 5 Mrad radiation before and after irradiation is shown in Figures 22 and 23.

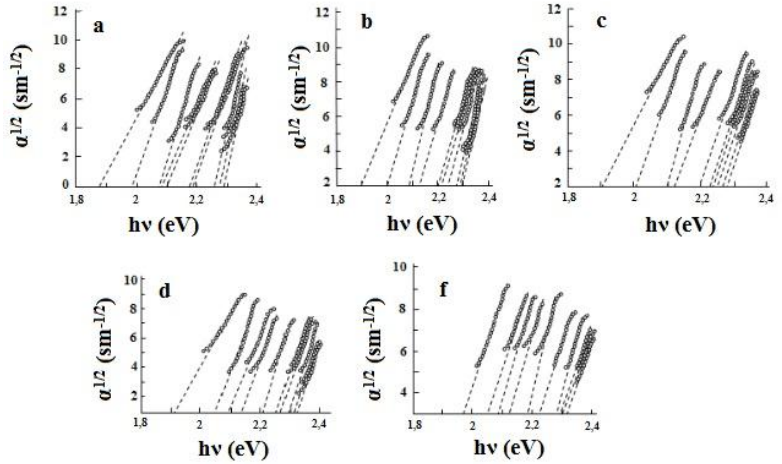

Figure 20. $TlGa_{1-x}In_xSe_{2(1-x)}S_{2x}$(x= 0; 0,1; 0,2; 0,3; 0,4; 0,6; 0,7; 0,8; 0,9; 1,0) dependence of the across absorption spectrum of systemic solid solutions on the diagonal at room temperature from the energy of the photon (a- 0 MGy, b- 0.01 MGy, c- 0.02 MGy, d- 0.05 MGy, f- 0.25 MGy).

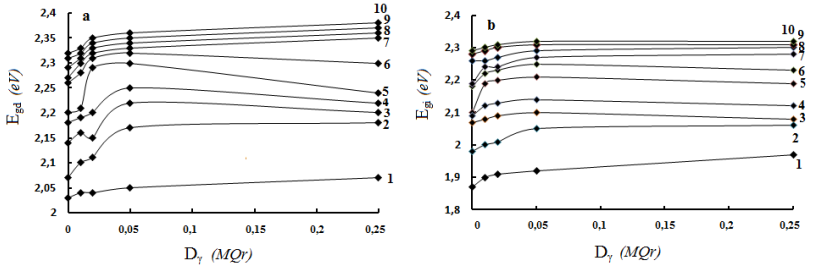

Figure 21. $TlGa_{1-x}In_xSe_{2(1-x)}S_{2x}$ (1- x=0; 2-x=0,1; 3-x=0,2; 4-x=0,3; 5-x=0,4; 6-x=0,6; 7-x=0,7; 8-x=0,8; 9-x=0,9; 10-x=1,0) before and after irradiation of solid solution samples, concentration-dependent curve of the straight and across of width of the for-bidden band.

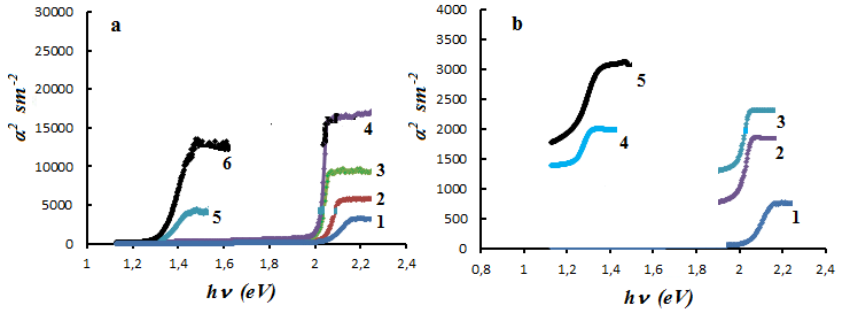

Figure 22. $TlGa_{1-x}In_xSe_2$ (x= 0; 0,1; 0,2; 0,3; 0,9; 1,0) is the dependence of the absorption spectrum of the systemic solid solutions on the energy of the photon at room temperature (a- 0 MGy, b- 0.05 MGy).

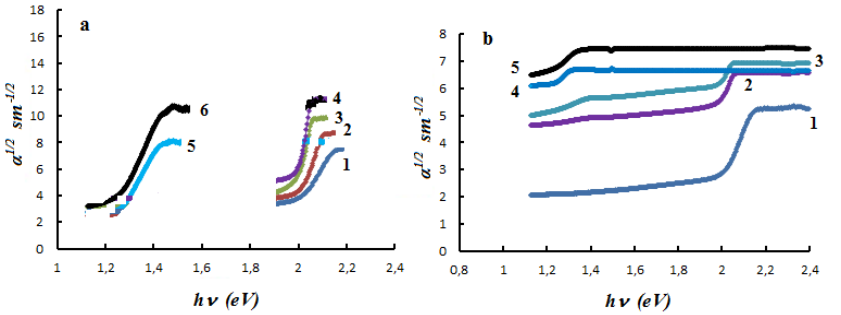

Figure 23. $TlGa_{1-x}In_xSe_2$ (x= 0; 0,1; 0,2; 0,3; 0,9; 1,0) dependence of the across absorption spectrum of systemic solid solutions on the diagonal at room temperature from the energy of the photon (a- 0 MGy, b-0,05 MGy).

The concentration dependence of the values of the width of straight and cross forbidden band of the samples of solid solutions $TlGa_{1-x}In_xSe_2$ (x= 0; 0,1; 0,2; 0,3; 0,7; 0,8; 0,9; 1,0) irradiated at 0 MGy and 0.05 MGy is given in Table 3. As can be seen from the dependence of the absorption coefficient on the photon energy, the linear absorption varies significantly in the solid solution compared to the foreign content in the solid solution under study.

Table 3.

The concentration dependence of the values of the width of straight and cross forbidden band of the samples of solid solutions $TlGa_{1-x}In_xSe_2$ (x= 0; 0,1; 0,2; 0,3; 0,7; 0,8; 0,9; 1,0) irradiated at 0 MGy and 0.05 MGy

Tərkib	E_{gd}(eV)	E_{gi}(eV)	E_{gd}(eV)	E_{gi}(eV)
	0 MGy		0,05 MGy	
$TlGaSe_2$	2,05	1,98	2,15	1,9
$TlGa_{0.9}In_{0.1}Se_2$	2,14	1,957	-	-
$TlGa_{0.8}In_{0.2}Se_2$	2,0	1,95	1,95	1,74
$TlGa_{0.7}In_{0.3}Se_2$	2,0	1,9	1,9	1,61
$TlGa_{0.1}In_{0.9}Se_2$	1,32	1,21	1,16	0,8
$TlİnSe_2$	1,3	1,2	1,15	0,75

For $TlGa_{1-x}In_xSe_{2(1-x)}S_{2x}$ and $TlGa_{1-x}In_xSe_2$ samples irradiated at doses of 0; 0.01; 0.02;0.05 and 0.25 MGy, the width of the straight and across forbidden band was calculated. In solid solutions of TlGa1-xInxSe2 (1-x) S2x and TlGa1-xInxSe2 systems, the concentration dependence of the width of the straight and across forbidden band from the reflection and emission spectra at room temperature in the range of 400-1100 nm was determined (Figure 17). It was found that the $TlGa_{1-x}In_xSe_{2(1-x)}S_{2x}$ system increases the width of the forbidden band with increasing concentration and radiation dose in solid solutions. In solid solutions of $TlGa_{1-x}In_xSe_2$, the width of the forbidden band decreases with increasing radiation dose [2, 5, 10, 13, 16 22].

MAIN RESULTS

1. The electrical conductivity of $TlGa_{1-x}In_xSe_{2(1-x)}S_{2x}$ and $TlGa_{1-x}In_xSe_2$ system solid solutions irradiated with γ-quanta in the temperature range of 300-100 K was studied and the temperature ranges of the presence of jumping conductivity were determined. Within the Mott approximation, the values of the parameters of the jumping conductivity were calculated, and the dependence of the concentration and radiation dose was determined: for a solid solution of $TlGa_{1-x}In_xSe_{2(1-x)}S_{2x}$, the density of localized states near the Fermi level is 0 -0,75 MGy N_F - $3{,}71 \cdot 10^{17}$-$3{,}79 \cdot 10^{18}$ $eV^{-1} \cdot sm^{-3}$, increase in the concentration of traps N_t - 0 -0,75 MGy $3{,}04 \cdot 10^{16}$-$1{,}66 \cdot 10^{17} sm^{-3}$ depending on the composition and radiation dose, the average length of the jumps R- 0 MGy $-1{,}72 \cdot 10^{-6}$-$1{,}5 \cdot 10^{-6}$sm; 0,25 MGy $-1{,}51 \cdot 10^{-6}$-$1{,}04 \cdot 10^{-6}$sm; 0,75 MGy $-1{,}34 \cdot 10^{-6}$-$9{,}77 \cdot 10^{-7}$sm; 0.75 MGy -1.34 • 10-6-9.77 • 10-7cm and and a decrease in the energy difference values of localized cases was determined - ΔE - 0 MQr -0,082-0,07 eV; 0,25 MGy -0,077-0.05 eV; 0,75 MGy -0,059-0,044 eV.

2. It has been determined that the current in the nonlinear part of the Volt-Ampere characteristics of $TlGa_{1-x}In_xSe_{2(1-x)}S_{2x}$ and $TlGa_{1-x}In_xSe_2$ systemic solid solutions exposed to γ-radiation is due to the weak field effect and it is explained in the context of Pool-Frenkel's heat-field theory. It has been shown that as the radiation dose increases, the value of the trap concentration (N_t) increases, while the free path length (λ), Frenkel coefficient (β) and distance from the traps to the maximum of the potential fence (x_m) decrease

3. It was found that the temperature dependence of the electrical conductivity of samples of solid solutions of $TlGa_{1-x}In_xSe_{2(1-x)}S_{2x}$ and $TlGa_{1-x}In_xSe_2$ irradiated with γ-quanta (σ (T)) at room temperatures above room temperature is related to the transition to the superion state of the crystal. A mechanism explaining the observed nature of conductivity has been proposed and it has been shown that the observed ionic conductivity is related to the diffusion of Tl^+ ions in vacancies in the thallium sublattice.

4. The frequency dispersion of the dielectric permittivity of the solid solution of the system $TlGa_{1-x}In_xSe_{2(1-x)}S_{2x}$ and $TlGa_{1-x}In_xSe_2$ irradiated with γ-quanta and the relaxor properties of the dielectric loss angle were determined. The parameters of a given conduction mechanism were evaluated before and after γ radiation. It was found that the increase in conductivity with a jump at 10^6 Hz is due to the transition of the system to superion.

5. Complex impedance spectra were studied in non-irradiated and γ-quantum irradiated $TlGa_{1-x}In_xSe_{2(1-x)}S_{2x}$ and $TlGa_{1-x}In_xSe_2$ systemic solid solutions. It was determined that the impedance obtained after γ-radiation is the result of the Warburg diffusion impedance from the hodograph curves. The rays in the impedance diagram are related to Warburg's diffuse impedance, which is based on the fact that the sinusoidal signal of a given ion carrier cannot reach the diffusion layer boundary in the frequency range.

6. In solid solutions of $TlGa_{1-x}In_xSe_{2(1-x)}S_{2x}$ and $TlGa_{1-x}In_xSe_2$ systems exposed to γ-radiation, at room temperature in the spectral range of 400-1100 nm, concentration dependence of the width of the forbidden band on the straight and across of the reflection and emission spectra was determined. It was found that in solid solutions $TlGa_{1-x}In_xSe_{2(1-x)}S_{2x}$ the width of the forbidden zone increases with increasing concentration and radiation dose, while in solid solution $TlGa_{1-x}In_xSe_2$ the width of the forbidden zone decreases after irradiation: with increasing x, respectively 0 MGy - E_{gd} = 2.04-2.35 eV; E_{gi} = 1.88-2.285 eV: 0.01 MGy - E_{gd} = 2.01-2.34 eV; E_{gi} = 1.89-2.3 eV: 0.02 MGy-E_{gd} = 2.01-2.31 eV; E_{gi} = 1,895-2.29 eV: 0.05MGy - E_{gd} = 2.02-2.3 eV; E_{gi} = 1.95-2.27 eV: In solid solution $TlGa_{1-x}In_xSe_2$, the width of the forbidden zone decreases after irradiation: 0 MGy E_{gd} = 2.05-1.3 eV; E_{gi} = 1.98-1.2 eV: 0.05 MGy E_{gd} = 2.15-1.15 eV; E_{gi} = 1.9-0.75 eV was observed

7. The study of the electrical conductivity of the non-irradiated and γ-quantum irradiated $TlInS_2$<V> crystal under the influence of an alternating electric field showed that when the system is in a relaxed state (irregular phase), ie in the range of Burns (T_d) and Fogel-Fulcher temperatures bears. The values of the burst conductivity pa-

rameters were calculated: the values of localized density (N_F), trap concentration (N_t) increased depending on the additive and radiation dose, and the values of average burst length (R) and localized energy difference (ΔE) decreased.

8. Studies of $TlInS_2$ and $TlInS_2$ <0.1%V>crystals and $(TlGaSe_2)_{1-x}(TlInSe_2)_x$ solid solutions by the Atomic Force Microscope method have shown that, the effects of radiation increase the saturation of nanoscale clusters, increase the ability of molecules to dissociate, and lead to the formation of critical embryos.

THE MAIN RESULTS OF THE DISSERTATION ARE PUBLISHED IN THE FOLLOWING ARTICLES AND THESISES

1. Sardarly R.M. Space charge-induced polarization and ionic conductivity in $TlInSe_2$ / R.M. Sardarly, O.A. Samedov, N.A. Alieva, A.P Abdullayev, E.K Guseinov, I.S Hasanov., F.T. Salmanov / Physics and technology of semiconductors**,** -2014, т. 48, в.4, -с.442-447
2. Salmanov F.T., Aliyeva N.A., Mikayilova A.J. Optical properties of solid solutions of $(TlGaSe_2)_{1-x}(TlInS_2)_x$ system in fundamental absorption region // Materials of the second international scientific-practical conference "The role of young scientists in the development of science, innovation and technology", -Dushanbe, Tajikistan, -11-12 may, -2017, -s.326-327.
3. Salmanov F.T. The effect of γ-rays on the electrical and dielectric properties of $TlInS_2$ crystals doped with vanadium atoms / Salmanov F.T., N.A. Alieva // ANAS Young Researcher scientific-practical journal. -2017, III, №2, -p.20-26.
4. Сардарлы Р.М. Влияние интеркаляции <V> на релаксорные свойства кристаллов $TlInS_2$ / Р.М. Сардарлы, О.А.Самедов, Ф.Т. Салманов // Azərbaycan Respublikası Təhsil Nazirliyi Azərbaycan Texniki Universitetinin Elmi əsərləri, -2017, №3, -s.53-56
5. Salmanov F.T. Influence of γ -radiation on direct and indirect optical transitions in $(TlGaSe_2)_{1-x}(TlInS_2)_x$ mixed crystal // Journal of Radiation Research, - 2018, v 5, №2, -s.457-464
6. Salmanov F.T. $TlInS_2$ və $TlInS_2$ <V> kristallarının Van-Der-Vals səthinin atom qüvvə mikroskopu ilə tədqiqi // Azərbaycan Respublikası Təhsil Nazirliyi Azərbaycan Texniki Universitetinin Elmi əsərləri, -2018, №1, -s.26-32.
7. Sardarly Rauf. Phase Transition in TlS, TlSe and $TlInS_2$ Crystals Caused by Nanoscale Defects / Rauf Sardarly, Arzu Sardarli, Famin Salmanov, Nurana Aliyeva, Samira Gahramanova, Mahammed Yusifov // International Journal of Theoretical and Applied Nanoscience and Nanotechnology. - 2018.v.6, - p.5-10.
8. Salmanov F.T. γ-kvantlarla şüalanmış (TlGaSe2)1-x(TlInSe2)x (x=0; 0,1; 0,2) bərk məhlullarının atom qüvvə mikroskopu ilə səth proseslərinin tədqiqi / F.T. Salmanov, N.Ə.Əliyeva,

C.H.Cabbarov, G.E.Məmmədova, R.A.Məmmədov, İ.A.Abdullayeva, S.D.Dadaşova // Gənc Tədqiqatçı, Fizika-riyaziyyat və Texniki elmləri, - 2018, IV cild, №2, -s.6-11.

9. Salmanov F.T., Aliyeva N.A., Mikayilova A.J., Abdullayeva I.A. Dielectric relaxation in gamma-irradiated of $(TlGaSe_2)_{1-x}(TlInS_2)_x$ solid solution // Международный форум молодых ученых «BURABAY FORUM: приграничное сотрудничество Казахстана», -Qazaxıstan, Astana: -06-13 avqust, - 2018,
10. Salmanov F.T. Influence of γ -radiation on direct and indirect optical transitions in $(TlGaSe_2)_{1-x}(TlInS_2)_x$ mixed crystal //Journal of Radiation Researches, - 2018, vol 5, №2, -s.457-464
11. Sardarly R.M. Impact of γ-irradiation on dielectric and electric properties of TlInS2 <V> crystals / R.M., O.A.Samedov, F.T.Salmanov, N.A.Aliyeva // ISSN (VANT), -2019, 120, 2, -p.30-33.
12. Sərdarlı R.M. γ-kvantlarla şüalanmış $(TlGaSe_2)1_{-x}(TlInS_2)_x$ bərk məhlullarının impedans xarakteristikaları / R.M. Sərdarlı, F.T. Salmanov, N.Ə. Əliyeva // AJP Fizika, -2019, vol. XXV, №2,-s.34-39.
13. Салманов Ф.Т.. Влияние γ-облучения на прямые и непрямые межзонные оптические переходы в кристаллах $TlGaSe_2$ и $TlInS_2$ // Azərbaycan Milli Elmlər Akademiyasının xəbərləri Fizika-texnika və riyaziyyat elmləri seriyası, fizika və astronomiya. – 2019, №2, -s143-148.
14. Salmanov F.T. İnfluence of γ-irradiation on supericonic conductivity of $(TlGaSe_2)_{1-x}(TlInS_2)_x$ solid solutions // Journal of Radiation Researches, -2019, vol.6 , №1,- s.5-10.
15. Салманов Ф.Т. АС-проводимость твердых растворов $(TlGaSe_2)_{1-x}(TlInS_2)_x$ // Gənc Tədqiqatçı, Fizika-riyaziyyat və Texniki elmləri, -2019, V, №1, -s.26-30.
16. Сардарлы Р.М., Салманов Ф.Т., Алиева Н.А., Маммадов Р.А. Тип оптических переходов на краю фундаментальново поглощения кристаллов $TlGaSe_2$ и $TlInS_2$, подвергнутых γ-облучению // Международный научный форум «Ядерная

наука и технологии», - Алматы, Казахстан, -24-27 June, -2019, -с.129-131.
17. Сардарлы Р.М. Прыжковая проводимость твердых растворов $(TlGaSe_2)_{1-x}(TlInS_2)_x$ / Р.М. Сардарлы, Ф.Т. Салманов, Н.А. Алиева // Azərbaycan Texniki Universiteti, -2019, №1, -s.11-18.
18. Сардарлы Р.М., Салманов Ф.Т., Алиева Н.А. Проводимостиь по локализованным состояниям твердых растворов $TlGa_{1-x}In_xSe_2$ // Релаксационные явления в твердых телах. Материалы XXIVмеждународной конференции, -Воронеж, -24-27 сентября, -2019, -с. 206-207.
19. Sardarli R.M., Salmanov F.T., Aliyeva N.A., Mammadov R.A. Superionic conductivity of $(TlGaSe_2)_{1-x}(TlInS_2)_x$ mixed crystals induced by γ-irradiation // Международный научный форум «Ядерная наука и технологии», -Алматы, Казахстан, -24-27 June, -2019, -s.70-71
20. Салманов Ф.Т., Алиева Н.А., Микаилова А.Дж., Маммадов Р.А. Импедансные характеристики γ-облученных твердых растворов $(TlGaSe_2)_{1-x}(TlInS_2)_x$ в радиочастотном диапазоне // «Пятый междисциплинарный молодежный научный форум с международным участием «Новые материалы», -Москва: -2019, -с 274-275.
21. Сардарлы Р.М. Импеданс Твердых Растворов $(TlGaSe_2)_{1-x}(TlInSe_2)_x$ / Р.М.Сардарлы, Ф.Т.Салманов, Н.А.Алиева // Azərbaycan Milli Elmlər Akademiyasının xəbərləri, Fizika-texnika və riyaziyyat elmləri seriyası, fizika və astronomiya, - 2019, №5, -s.56-64
22. Сардарлы R.M. Тип оптических переходов на краю фундаментального поглощения кристаллов $TlGaSe_2$ и $TlInS_2$, подвергнутых γ-облучению / R.M.Сардарлы, Ф.Т. Салманов, Н.А.Алиева // Оптика и спектроскопия, -2019, т. 127, в. 3, -с.420-424
23. Sardarly R.M. Impedance Spectroscopy Of $(TlGaSe_2)_{1-x}(TlInSe_2)_x$ Solid Solutions In Radio Frequency Range / R.M. Sardarly, F.T. Salmanov, N.A. Aliyeva, R.M.Abbasova // Modern physics letters b, -2020, V.34, n.11, -p.2050113.

24. Sardarly R.M. Импедансные характерстики γ-облученных твердых растворов $(TlGaSe_2)_{1-x}(TlInS_2)_x$ / R.M. Sardarly, F.T. Salmanov, N.A. Aliyeva, R.M.Abbasova // Физика и техника полупроводников, -2020, т. 54, в. 6, -с.511-518.

The defense will be held on **08 October** 2021 at **15^{00}** at the meeting of the Dissertation council BED 1.21 of Supreme Attestation Commission under the President of the Republic of Azerbaijan operating at the Institute of Radiation Problems of Azerbaijan National Academy of Sciences

Address: AZ1143, B.Vahabzadeh 9, Baku

Dissertation is accessible at the Institute of Radiation Problems of Azerbaijan National Academy of Sciences

Electronic versions of dissertation and its abstract are available on the official website of the Institute of Radiation Problems of Azerbaijan National Academy of Sciences

Abstract was sent to the required addresses on **07 September** 2021

Signed for print: 03.09.2021

Paper format: A5

Volume: 76412 characters

Number of hard copies: 30